#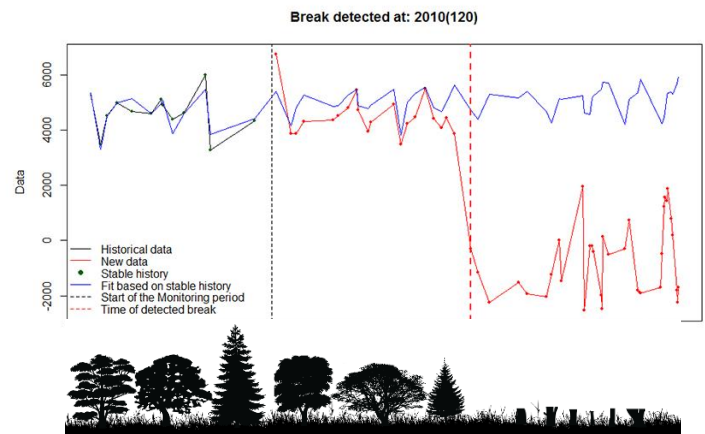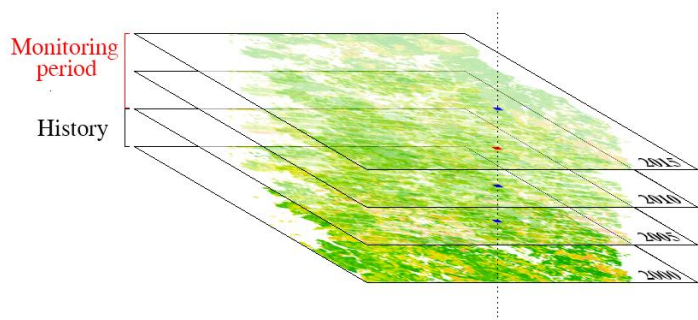 Detecting clear-cut deforestation using Landsat data: A time series analysis of remote sensing data in Covasna County, Romania between 2005 and 2015

Tudor Buhalău

Tudor Buhalău (2016).

Detecting clear-cut deforestation using Landsat data: A time series analysis of remote sensing data in Covasna County, Romania between 2005 and 2015

Master degree thesis, 30 credits in *Physical Geography and Ecosystem Analysis*

Department of Physical Geography and Ecosystem Science, Lund University

Level: Master of Science (MSc)

Course duration: *January* 2016 until *June* 2016

Detecting clear-cut deforestation using Landsat data: A time series analysis of remote sensing data in Covasna County, Romania between 2005 and 2015

Tudor Buhalău

Master Thesis, 30 credits, in *Physical Geography and Ecosystem Analysis*

Supervisor 1

Daniel B. Metcalfe (Lund University)

Supervisor 2

Hongxiao Jin (Lund University)

Examiners:

Helena Eriksson (Lund University)

Harry Lankreijer (Lund University)

Abstract

Forested areas represent a fundamental component of the environment. Deforestation and forest fragmentation represent a global issue mostly caused by human influence and Romania is not an exception. Nowadays forests cover approximately a third of Romania's surface, meaning that the deforestation is a national issue. To handle this problem, a monitoring tool is necessary.

The aim of the present study is to detect clear-cut deforestation using time series analysis between 2005 and 2015 in Covasna County, Romania. To achieve this objective, the analysis focuses on solving three main issues: (i) assess if clear-cut deforestation can be detected in the study area, (ii) determine the spatio-temporal distribution of the clear-cut deforestation, and (iii) confront these results with the official deforestation rates.

A time series decomposition method (BFAST - Breaks For Additive Seasonal and Trend) has been used on Landsat imagery to detect forest cover changes. To identify the most suitable spectral index for detecting clear-cut deforestation, the algorithm was initially tested on a smaller test area. BFAST applied on Normalized Difference Moisture Index (NDMI) has been proved to have more consistent results than BFAST applied on Normalized Difference Vegetation Index (NDVI).

This study concludes that clear-cut deforestation can be detected using BFAST algorithm considering forest type and the scale of the study area. Between 2005 and 2015, in Covasna County, Romania, 1.71% of forest cover, representing 2953 ha, was deforested. Contrary to the official deforestation rate, that mainly shows an increase of the deforestation rate for the last 10 years, the results of this study present a decrease in clear-cut deforestation between 2005 and 2015. The detection process was estimated to have an overall accuracy of 84%.

Therefore, the presented method is a promising tool for monitoring clear-cut deforestation in Romania at national scale.

Keywords: deforestation, Covasna, BFAST, Landsat, time series, NDVI, NDMI

Preface

This thesis represents a continuation of my interests for both remote sensing and environmental sciences.

Since childhood, I am a nature enthusiast. My interest for maps and environment was nurtured by the Scouts d'Europe, where I have been a key member for my whole life. I consider that scouting had not only developed my ecologist nature, but also my teamwork spirit.

The chosen study area has a personal significance, being close to my hometown. Growing up with the mountains in the neighbourhood, I spent most of my childhood in the near forests. Years after, when I have returned with my mountain bike, I had the unpleasant surprise to discover that the road, once surrounded by forest, was now at its edge. This was my inner motivation to start on this journey that became my master thesis.

After a week of staring blank at an almost empty page with only the "Preface" title on it, I understand why it is the last and hardest chapter to write. It doesn't only rewind every article or book you read, but you relive the challenges and tough decisions that were ultimately the building blocks of this thesis.

I would like to express my gratitude to my supervisors, Dan Metcalfe and Hongxiao Jin, and my home university supervisor, Cristian Vasile, for their support and guidance throughout my thesis.

I would also like to thank the Erasmus+ Programme with the coordinators Ecaterina Ștefan (Erasmus institutional coordinator at University of Agronomic Sciences and Veterinary Medicine of Bucharest), Paul Miller (International Coordinator, INES) and Raluca Manea (Dean of Faculty of Land Reclamation and Environmental Engineering).

Lastly, I want to thank my family, my friends, Andrei Mîrț and Sabina Roșca, for their guidance in R environment, and my colleague Luana Andreea Simion, who made me feel closer to home in this mobility.

Lund, June 2016

Contents

List of Figures

List of Tables

List of Abbreviations

AOI	Area of interest
BFAST	Breaks For Additive Seasonal and Trend
BT	Brightness Temperature
CUSUM	Cumulative Sum
ETM	Enhanced Thematic Mapper
GHG	Greenhouse gas
IFN	National Forest Inventory
LandTrendr	Landsat-based detection of Trends in Disturbance and Recovery
LEDAPS	Landsat Ecosystem Disturbance Adaptive Processing System
LTS	Landsat Time series Stack
MEaSUREs	Making Earth System Data Records for Use in Research Environments
MODIS	Moderate Resolution Imaging Spectroradiometer
MOSUM	Moving Sum
MRV	Measurement, Reporting and Verification
NA	Not Available
NASA	National Aeronautics and Space Administration
NDMI	Normalized Difference Moisture Index
NDVI	Normalized Difference Vegetation Index
NFMS	National Forest Monitoring Systems
NIR	Near Infra-Red
OLI	Operational Land Imager
REDD+	Reducing Emissions from Deforestation and Forest Degradation and the role of conservation, sustainable management of forests and enhancement of forest carbon stocks in developing countries
SAR	Synthetic Aperture Radar
SCD	Sub-annual Change Detection
SLC	Scan Line Corrector
SWIR	Short-Wave Infra-Red
TIRS	Thermal Infrared Sensor
TOA	Top Of Atmosphere
TAU	Territorial Administrative Units
USGS	United States Geological Survey
USSR	Union of Soviet Socialist Republics

1. Introduction

1.1 Context

Forested areas represent a fundamental component of the environment, playing an important role in the global carbon cycle. In the context of climate change, forest management can be a powerful tool for reducing greenhouse gas (GHG) emissions, forests being one of the Earth's major carbon stocks (Lawrence and Nicoll, 2016). Between 1990 and 2015, the global forest area significantly reduced by 3% (Keenan et al., 2015) as a result of both deforestation and forest degradation. Although changes in species composition and diameter distribution, as well as reduced stocking density caused by natural elements, are an important factor in causing biodiversity loss and climate change (Pfaff et al., 2013), the public interest is more focused on deforestation (MacDicken, 2015), as human activity mostly influences it.

The world's forests can be divided into three major forest types: boreal, temperate and tropical, being delineated mainly by the geographic position, elevation and climate (Grebner et al., 2013). Considering the global distribution and species composition, temperate forests are continuously changing due to human activities, disease and climate (Willis, 2009).

Forests in general, but especially the European ones, cannot be entirely understood without assessing their past and their evolution in time. Nowadays, in Europe, anthropogenic footprints are obviously reflected, forests covering only 30% of Europe (Chertov et al., 2006). Still, unlike Western Europe's forests, the Carpathian forests remain relatively undisturbed, being rich in biodiversity (Knorn et al., 2012) – "the diversity of plant-life in the Balkans is richer than any comparable area in Europe" (Willis, 1994).

Throughout history, changes in forest management were influenced by political, socio-economic and institutional drivers (Munteanu et al., 2016). Romania has experienced multiple shifts in this respect, due to frequent regime changes from Austro-Hungarian, to Ottoman and Soviet, and later on, to European Union policy. The changes in ownership from private to public property are also influencing the changes in forest cover in a negative way (Knorn et al., 2012). Between the end of World War II and 1960, the Romanian Forest Fund was overexploited to pay the war debts to USSR and, after the collapse of the Communism in 1989, the vulnerable system led to ambiguity in ownership, which finally leads to fragmentation and decrease of forested areas. The new democratic government of Romania, issued the law 18/1991, allowing restitution of land rights (abusively confiscated by the communist regime), for state-owned land parcels smaller than 1 hectare (Mihășan, 2009). This decision led to an even bigger fragmentation of the forest fund, much higher than before the nationalization of the forests (Curtea de Conturi, 2014). The main causes of illegal deforestation are connected with the fragmentation process, by means of the late implementation of the forest fund legislation as well as the absence of a stable system subordinated to the central authority responsible for forestry (Curtea de Conturi, 2014). The combination of political and economic drivers, influenced by corruption led to a vulnerable security system in forest management, which finally resulted in massive deforestation after 1989 (WWF Danube Carpathian Programme, 2005).

The Romanian Ministry of Environment and Forests declared that Romania had a total of 6,529,000 hectares of forest land in 2015, which also include the protected areas managed mostly by the National Forest Administration "Romsilva" (Knorn et al., 2012). Even if the official numbers of total deforested areas are lower than the permitted amount, deforestation is an issue, illegal logging being an attack on national security (DIGI 24, 2015).

1.2 Background

Remote sensing techniques are a successful tool for detecting forest cover change, starting with bi-temporal classifications of land use (change/no-change maps generated from two land-use maps created at two different moments in time) to time series analysis, which could be a solution for a better understanding of vegetation dynamics and for actively monitoring these changes.

The primary issues in forest dynamics analysis are detecting deforestation and also reforestation. In this study, detecting clear-cut deforestation is the main concern. Recently, several methods were developed for this purpose and they rely on the analysis of a succession of satellite images, which in scientific literature is known as a time series analysis.

One of these is Breaks For Additive Seasonal and Trend (BFAST) developed by Verbesselt et al. (2010a). This algorithm can use Moderate Resolution Imaging Spectroradiometer (MODIS) records (Lambert et al., 2015; Verbesselt et al., 2010a), Landsat records (Baumann et al., 2012; DeVries et al., 2015 Dutrieux et al., 2016; Hermosilla et al., 2015), or combination between them (Tran et al., 2016). Other methods such as the Landsat-based detection of Trends in Disturbance and Recovery - LandTrendr (Kennedy et al., 2010) or correlation between Synthetic Aperture Radar (SAR) and Landsat (Reiche et al., 2015) are also currently used.

In Romania, the LandTrendr algorithm was used to detect deforestation in the Transilvanian basin between 1984 and 2000 (Knorn et al., 2012). Although a real/near-real time deforestation monitoring program could be a valuable tool for monitoring illegal deforestation, unfortunately, such a program does not exist yet.

As it is the case all around the world, in Romania forest are affected by both natural and anthropic factors. The natural factors include pests, disease, soil erosion, fires (during very dry periods), strong winds and heavy snowfall. The principal anthropic influences upon the forests are the illegal or improper logging operations (Merce, 2012). It is important to mention that generally, in Romania, deforestation can be divided in two main parts: clear-cut (when all the trees are cut down) and selective (where the forest district employees choose which tree should be cut down, based on species, diameter, average quality of the tree and height). In the remote sensing field, detecting selective deforestation will be almost impossible (WWF Danube Carpathian Programme, 2005).

1.3 Problem definition

In Romania, the forests mostly surround the Carpathian Mountains, all of the mountain areas being threatened by both legal and illegal deforestation. The most influenced counties are Dâmbovița, Argeș, Bacău, Olt, Mehedinți and Covasna (WWF, 2016). Being situated in the Eastern Carpathian group, with about 46% of its surface covered by both deciduous and coniferous forest (RoSilva, 2016) and being entirely covered by a single Landsat scene (i.e. path 183, row 28), Covasna County represents an optimal area to conduct an exploratory study on detecting clear-cut deforestation based on time series analysis, which can afterwards be extended to national scale.

Although being a pressing matter with deep economic, social and ecologic implications, deforestation barely makes the cut for the priorities agenda of Romania's Government. Currently, there is no systematic registration (cadastre) of the whole country. Land-use maps are produced by visual interpretation and vectorization of aerial imagery by CNGCFT (National Centre of Cartography) (National Cartography Center History, 2016).

In Romania, the forest monitoring system is confusing, various small agencies handling small areas with no support from the Ministry to manage them all together. The IFN (National Forest Inventory), founded in 2006, aims to provide an inventory every five years, combining photogrammetry and field data. The first inventory was conducted between 2008 and 2013, and the next one will be finished in 2018 (Nostra Silva, 2016). Thus, with a five-year cycle, it is hard to identify, trace and verify the legitimacy of deforestation. A more often inventory, for example at one-year cycle might improve the previously mentioned problems.

1.4 Research objective and research questions

The aim of this thesis is to detect clear-cut deforestation in Covasna County, Romania, using Landsat time series data sets from 2000 to present.

To achieve this, the following research questions have to be answered:

RQ 1. Can deforestation in Covasna, Romania, be detected using BFAST?

   SRQ1.1 How to translate change to detected clear-cut deforestation?

   SRQ1.2 What spectral index is most suitable to detect clear-cut deforestation?

RQ 2. What is the spatio-temporal distribution of clear-cut deforestation between 2005 and 2015 in Covasna County, Romania?

RQ 3. What is the difference between the detected clear-cut deforestation and the official deforestation rate in Covasna County, Romania?

2. Literature review and theoretical background

2.1 Detecting deforestation at national scale

As presented in Introduction, deforestation leads to multiple negative effects. All around the world, there are various monitoring systems that make it possible for deforestation to be detected and therefore reduce these threats. In order to detect forest change, three main tools can be used: ground-based, satellite-based, and airborne (Davis and Petersen, 2016), each having different usage, depending on scale. Below are presented a few examples of how different countries handle this issue.

Systems as PRODES (Projeto de Monitoramento do Desmatamento na Amazônia Legal por Satélite) (PRODES, 2016) and DETER (Sistema de Detecção do Desmatamento em Tempo Real na Amazônia) (Deter, 2016), coordinated by the Brazilian Space Agency (INPE), are used for monitoring the near real-time deforestation and mapping the annual deforestation (DeVries et al., 2015b).

Also, the "Reducing Emissions from Deforestation and Forest Degradation and the role of conservation, sustainable management of forests and enhancement of forest carbon stocks in developing countries" (REDD+) mechanism is used to adopt national strategies for reducing emissions from deforestation and forest degradation in developing countries with tropical forests (The REDD Desk, 2016). Through this mechanism, developing countries are financially compensated for afforestation and for keeping existing forests undisturbed, forests that are fundamental for reducing global warming (The REDD Desk, 2016). "For the farmer that he can make money or more money from not cutting the tree than for cutting the tree, that is the idea of REDD+" Arild Angelsen – Professor, The Norwegian University of Life Sciences. Three phases define the REDD+ programme: Phase 1 defines policies and measures that a country needs to apply for implementing the program; Phase 2 implements demonstration activities and managing the REDD+ strategies; Phase 3 scales up the program at national level and implements the monitoring system, which ensures that the emission reduction is real (Food and Agriculture Organization of the United Nations, 2016).

In Romania, a program called „Radarul Pădurilor" (*Forest Radar*) was implemented by the Government in October 2014 (Government decision no. 470/2014) which states that every citizen can verify if a logging transport is legal by calling the emergency number 112 (Mediafax, 2016). With the support of an initiative that encourages afforestation, "Plantăm fapte bune în Romania" (*Planting good deeds in Romania*) an application called „Harta defrișărilor" (*Map of deforestation*) was released for Android users, where every user can add photos of a certain deforested area together with the GPS coordinates (Green Report, 2016). In addition, Greenpeace Romania initiated a crowdsourcing campaign in 2015 to recruit volunteers for collecting information about deforested areas and prevent further deforestation (Greenpeace, 2016).

2.2 Time series Analysis

Time series data are successfully used in fields like medicine, earth sciences, and economy (Chen et al., 2012). A time series represents a set of data collected at successive times, which may be distributed at constant time intervals. Time series analysis comprises several algorithms for analysing the data to obtain statistic information or other typical features of the data (Ramsey, 2012).

Many time series methods were developed over the years. These use both moderate and high spatial resolution (MODIS and Landsat, respectively) in order to detect all type of changes in the vegetation cover. Some of the most relevant factors that influence the results of a time series analysis are: frequency of satellite images, cloud cover and seasonality.

The Sub-annual Change Detection (SCD) algorithm (Cai and Liu, 2015) was used on a study site in Ohio USA, which detects dates of abrupt change from a succession of frequently recorded satellite images (e.g. 16 days MODIS or Landsat). The SCD approach analyses the differences noticed at intervals of two consecutive annual segments, in two phases. First, the initial time series is divided into many time series with a one-year temporal resolution and after that, the resulted time series are compared to detect differences between neighbouring years. In the second phase, the algorithm determines the points that do not follow the seasonal model. The authors state that the computation time of SCD algorithm take less than the BFAST method but it cannot make the difference between trend and seasonality.

Another method was developed by Kennedy et al. (2010), which introduced a new method for extracting spectral trajectories of land changes, from a Landsat Time series Stack (LTS), called Landsat-based detection of Trends in Disturbance and Recovery (LandTrendr). The method captures the short-duration events and smoothens the long-term trends. They state in their study that the change is not just a simple contrast between the condition of two points in time, but that the landscapes are influenced by the processes that are operating at fast and slow rates (Kennedy et al., 2010). The second part of the study was to calibrate and validate data for forest change detection algorithm with a tool called "TimeSync". They also state that the algorithm is appropriate for detecting disturbances and recovery phenomena.

The method that was chosen for this study is BFAST, as it has been used so far in various locations all around the world. Its flexibility is enhanced by different types of land use on which it was used, as presented in the next paragraphs.

BFAST is a method developed in 2010 that breaks up a time series into *trend*, *seasonal* and *remainder* components (Verbesselt et al., 2010a). This method can be applied to different remote sensing data (e.g. MODIS, Landsat) to detect and characterize changes, being used to provide information about the spatial and temporal position of the changes. It is important to use all available images from all months in order to determine a stable history and later to know exactly when is the time when deforestation occurs. This method was successfully used in Australia, to estimate the time and the magnitude of change in forested areas (Verbesselt et al., 2010a) (Figure 1.A).

6

Figure 1. World map indicating the locations where the BFAST algorithm was used (A- Australia - Verbesselt et al., 2010a, B- Somalia- Verbesselt et al., 2010b, C- France– Lambert et al. 2013, D- Mongolia- Tsutsumida et al. 2013, E- Australia- Watts and Laffan 2014)

Later, also in 2010, the main author makes an improvement in the algorithm, adding a harmonic seasonal model, which can be used with fewer observations. The harmonic seasonal model characterizes phenological change easily and is more robust against noise (Verbesselt et al., 2010b). In 2012, the same main author developed an improvement in the BFAST algorithm called BFAST Monitor (i.e. study area in Somalia) (Figure 1.B). To apply the algorithm to a time series, a moment that splits the time series into two parts is defined. The first period, called history period, is considered stable, where no change has occurred in land cover. The second, monitoring, period is where land cover change is detected. The algorithm fits a regression model to the data in the stable history period, that is then used to determine whether the observations in the monitoring period conform to this stable regression model or if any change is detected (Verbesselt et al., 2012b).

Lambert et al. (2013) present a study in France (Figure 1.C) from 2000 to 2012, where they compare the BFAST method with a phenological approach that was aimed to average the Normalized Difference Vegetation Index (NDVI) profiles, from a given period, in order to establish for each forest stand a mean phenological profile. The main tree species that were analysed were *Abies alba* (silver fir) and *Picea abies* (Norway spruce). The authors state that the two approaches give the same results regarding the trend. They also state that the BFAST approach is able to detect breaks in the linear trend but it is extremely difficult to use it to detect breaks in clear-cut areas that measure less than one hectare. This study is a relevant example of how clear-cut deforestation within coniferous forests (especially silver fir and Norway spruce species) can be detected using the BFAST algorithm.

In their paper, Tsutsumida et al. (2013) (Figure 1.D) successfully used the BFAST method to analyse the expansion of the urban area of Ulaanbaatar, the capital of Mongolia, during the period 2000-2010. They state that this tool can be used to monitor the urban expansion, being a robust and applicable method for this type of land use, thus confirming that it is adaptable to various types of land cover.

In their study, Watts and Laffan (2014) used the BFAST in a semi-arid region, in New South Wales, Australia (Figure 1.E). The study aimed to test the effectiveness of the algorithm in this type of region. In their case, the algorithm was able to detect changes in the vegetation greening caused by floods, but was not able to accurately detect fires (only 3%). In this study the spectral index used was EVI (Enhanced Vegetation Index), which indicates that the algorithm is able to use different kinds of spectral indices. With regard to the time series use, Watts and Laffan (2014) mentioned that "Such methods provide advantages over traditional bi-temporal change detection, as they are not scene dependent and use data with a finer temporal resolution".

2.3 Theoretical background

For the methodology to be better understood, several notions such as *Landsat, surface reflectance, cloud mask, spectral indices* and *forest cover* will be further explained in this section.

2.3.1 Landsat

In 1972, the first Landsat satellite was launched. Since then, Landsat continuously provided data for various fields such as environmental sciences and management, land use and land cover, agriculture, planning and development, economy, education, human needs, legal/security, oil/gas/mineral (Landsat USGS, 2016a).

Currently, the Landsat constellation has two functional satellites: Landsat 7, Enhanced Thematic Mapper Plus (ETM+), and Landsat 8, Operational Land Imager (OLI), the last one being launched in February 2013. The production of Landsat 9 already started, the satellite being scheduled to launch in 2023 (Landsat USGS, 2016a).

Landsat 7 ETM+ was launched in April 1999 and was designed with eight spectral bands including one thermal and one panchromatic band, with a temporal resolution of 16 days, and scene size 170 km x 185 km. After May 2003, all the scenes collected by Landsat 7 ETM+ cover only 78% of the image due to Scan Line Corrector (SLC) sensor failing. This failure leads to gaps that are not recoverable, being generated by a combination of its sun-synchronous orbit and side-to-side sweeping. Several software products can fill these gaps. Alternatively, United States Geological Survey (USGS) SLC-off Gap Mask could be downloaded to exclude affected data (Landsat USGS, 2016b).

Landsat 8, the latest satellite launched, has two sensors: OLI, with nine spectral bands including a panchromatic band, and Thermal Infrared Sensor (TIRS) with two spectral bands. The temporal resolution is 16 days with an 8-day offset from Landsat 7, and the scene size is 170 km x 185 km (Landsat USGS, 2016a).

2.3.2 Surface reflectance

Landsat surface reflectance, for both Landsat 7 and Landsat 8, is a high-level data product, provided directly by USGS. For Landsat 7 ETM+, the Landsat Ecosystem Disturbance Adaptive Processing System (LEDAPS) software is used to produce surface reflectance. The software was developed by Masek et al. in 2006 with the support from National Aeronautics and Space Administration *(*NASA). Making Earth System Data Records for Use in Research Environments (MEaSUREs), and it applies

MODIS atmospheric correction to the Landsat 7 Level 1 data products. The software uses digital elevation, geopotential height, water vapour and aerosol optical thickness as input data, to create surface reflectance, Top Of Atmosphere (TOA), and the mask for clouds and cloud shadows (Landsat USGS, 2016b).

The Landsat 8 Surface Reflectance (L8SR) algorithm is different from LEDAPS, by using the scene centre to calculate the sun angle, and hardcoding the zenith angle to zero. The cloud mask is produced using both OLI and TIRS (Landsat USGS, 2016b) sensors.

As the actual values of the spectral indices of the pixels can be affected by various factors (e.g. cloud cover and humidity), it is important to use high-level data products such as the ones mentioned above in order not to obtain anomalous results (Landsat USGS, 2016b).

2.3.3 Clouds

Clouds are one of the biggest problem in the remote sensing field and, therefore, masking the clouds and clouds shadow is one important step in time series analysis.

In 2012, Zhu and Woodcock developed the "Fmask" algorithm, which can detect clouds and cloud shadows for Landsat imagery. This method uses the TOA reflectance for Bands 1-7, except Band 6, for which the Brightness Temperature (BT) is used, generated by the LEDAPS software (Zhu and Woodcock, 2012). The 2015 Fmask comes with some improvements and it also covers Landsat 8. The same Landsat 4-7 algorithm is also used for Landsat 8, but the cirrus probability is calculated using the cirrus band instead (Zhu et al., 2015).

2.3.4 Spectral indices: NDVI and NDMI

The spectral indices are results of the combination of two or more spectral bands, which are indicating the relative abundance of various features of interest (Harris Geospatial, 2016).

The NDVI is one of the most successfully used vegetation spectral index. One of the reasons is that it allows comparison between inter-annual and seasonal changes in vegetation. The NDVI represents a ratio between the Near Infra-Red (NIR) and the Red bands (Huete et al., 2002). For Landsat 7, bands 4 (NIR) and 3 (Red) are used, while for Landsat 8, bands 5 (NIR) and 4 (Red) are used (USGS, 2015).

$$\text{NDVI} = \frac{NIR - R}{NIR + R}$$

Another successfully used index is the Normalized Difference Moisture Index (NDMI), which represents the ratio between two infra-red bands, NIR and Short-Wave Infra-Red (SWIR). For Landsat 7, bands 4 (NIR) and 5 (SWIR) are used and for Landsat 8, bands 5 (NIR) and 6 (SWIR) are used (USGS, 2015).

$$\text{NDMI} = \frac{NIR - SWIR}{NIR + SWIR}$$

2.3.5 Global Forest Watch

Global Forest Watch (GFW) is a monitoring network established in 1997, which aims at collecting and providing information to better understand, manage and conserve the forested landscapes. GFW includes near real-time alerts that display suspected location of recent forest cover loss. The GFW database also contains data about previously forest covered areas. In which the used methodology is concerned, the GFW recognizes only the trees that have a minimum height of 5 meters. The degradation process is not included in the GFW database, an example being the selective removals from the forests. The engine used for the forest dynamic monitoring is Google Earth Engine that combines public data with a large scale computational facility that processes the geospatial data. The pre-processing stages of the Landsat data (i.e. Landsat 4, 5, 7, 8) include: cloud, shadow and water screening as well as quality assessment and image normalization (Hansen et al., 2013).

3. Methodology

3.1 Study area

3.1.1 General

Covasna County (Figure 2) is located in the Eastern Carpathians group, between 45˚35' and 46˚18' N and 26˚4' and 26˚5' E, covering a total area of 3,710 km^2, which represents about 1.6% of Romania's surface (National Institute of Statistics, 2016a). The primary industries of Covasna County are timber, textiles, and food (Global Britannica, 2016).

The topography of Covasna is more than 50% mountains, with the rest being plains and foothills, altitude ranging from 468 m (Baraolt Valley) to 1,777 m (Lăcăuți Peak in Brețcului Mountains). Most of the soils are brown, brown podzolic and brown acid, especially in the mountain areas, and chernozem and brown podzolic in the lower altitude areas (ISU Covasna, 2014; National Institute of Statistics, 2016a). The hydrographic network is represented by Olt and Negru rivers and their affluents, which collect more than 1,000 springs, and three major lakes: Reci, Moacsa and Belin (Watercore, 2016). The climate in Covasna is temperate-continental, with cold and dry winters and hot summers. The precipitation values vary from 500 to 700 mm/year and the medium annual temperature is between 3 and 8 degrees Celsius (Watercore, 2016). In Covasna County, there are three protected areas: Mestecănişul Reci – 291 ha, Luci – 297.7 ha and Vârghişului – 198.7 ha. Within these protected areas, some regions are state-owned (RoSilva, 2016).
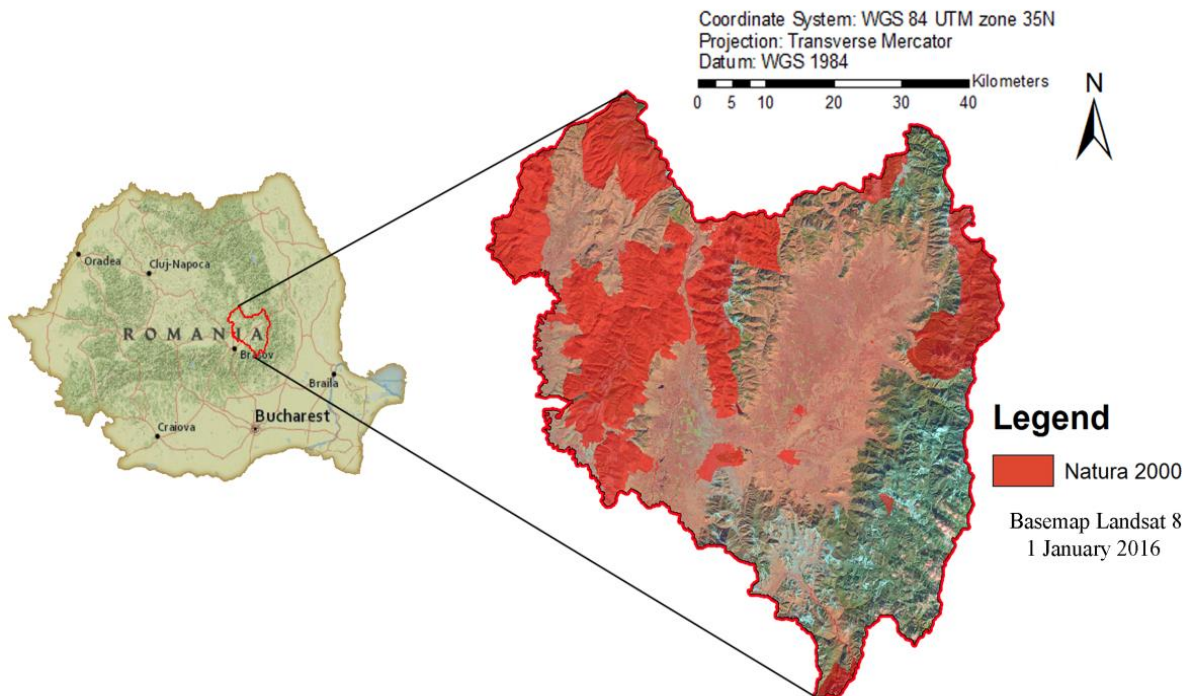
Figure 2. Geographic location of the study: Covasna County, Romania (map on the left: Romania, ESRI Basemap, National Geographic Word Map, map on the right: basemap Landsat 8- 1 January 2016 and Natura 2000 layer)

3.1.2 Forest type

According to the Ministry of Environment and Forests, the forest area of Romania is 6,529,000 ha (in 2015), representing 27.3% of Romania's total surface (Ministry of Environment and Climate Change Romania, 2016). The forests of Covasna County cover 46% of the total county area, representing 173,000 ha (RoSilva, 2016). The National Institute of Statistics states that the forested area in Covasna increased from 2000 (161,900 ha) to 2014 (171,300 ha). In 2014, 67,400 ha were coniferous species, 102,200 ha were deciduous species, and 1,700 ha being defined by another type of land use (National Institute of Statistics, 2016a). "Natura 2000" Network covers some of the forested areas in Covasna County, protecting both existing birds and habitats (EU Natura 2000, 2016).

The representative species of the forested areas are Norway spruce - *Picea abies*, silver fir - *Abies alba* (Figure 3), beech - *Fagus silvatica* (Figure 3), birch - *Betula pendula*, hornbeam - *Carpinus betulus,* oak varieties - *Quercus*, pine varieties – *Pinus* and juniper varieties - *Juniperus* (Bartha et al., 2015; Griffith et al., 2012).

The following pictures were taken near Ghelința and Pasul Oituz Covasna, with a Canon (PowerShot A2500, Tokyo, Japan) camera on the 15th of April 2016.

Figure 3. Pictures taken near Ghelința and Pasul Oituz Covasna, with a Canon (PowerShot A2500, Tokyo, Japan) camera on the 15th of April 2016 representing: silver fir (left) and beech (right)

3.2 Breaks For Additive Seasonal and Trend

The present study detects clear-cut deforestation from Landsat time series data by applying the BFAST algorithm developed by Verbesselt et al. (2010a). As described by the authors, BFAST is a decomposition method, which breaks a time series into *trend*, *seasonal* and *remainder* components (Figure 4). Changes in the *trend* component reveal disturbances such as fires and insect attacks while changes into the *seasonal* component reveal phenological changes such as changes in land cover type. The changes to which ecosystems are usually predisposed can be classified into three classes: seasonal, gradual and abrupt changes (Verbesselt et al., 2010a). The authors explain that the

seasonal changes are influenced by the temperature and rainfall interactions, which have an impact to plant phenology. The gradual changes are correlated with the interannual climate variability and gradual change in land degradation or management. The abrupt changes are the result of deforestation, urbanization and fires. The *remainder* consists in the remaining data variation aside from the seasonal and trend components (Verbesselt et al., 2010a).

The general equation for BFAST is: $Y_t = T_t + S_t + e_t$, t=1,…n where Y_t represents the observed data at time t, T represents the *trend*, S *seasonality* and e the *remainder* (Verbesselt et al., 2010a).
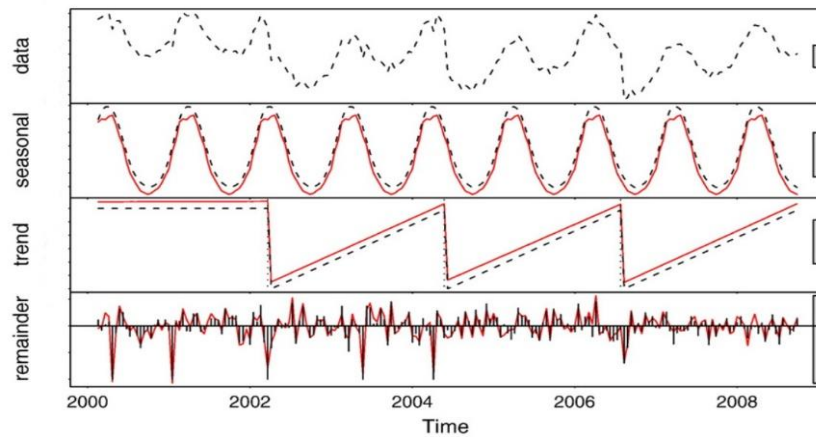
Figure 4. An example of a time series decomposition in Australia (2010) for the 2000 - 2009 period: data, seasonal, trend and remainder components (Verbesselt et al., 2010a)

3.2.1 BFAST Monitor

BFAST Monitor is a near-real time disturbance monitoring approach, which can be applied to various time series and uses the BFAST algorithm. The method was successfully used by Verbesselt et al., (2012) in drought-stressed regions in Somalia and by DeVries et al., 2015 in a tropical montane forest in southern Ethiopia. The method is developed to be used with any newly acquired data, being able to automatically identify and model a stable history, and afterwards detect the changes in the most recent data (Verbesselt et al., 2012b). The main advantages of this method are short processing time, not needing a vegetation-specific threshold, and not requiring techniques of gap filling (e.g. masked clouds), while still being able to successfully analyse the full temporal detail of a time series (Verbesselt et al., 2012b).

As described by DeVries et al., (2015), to classify changes in each pixel, BFAST algorithm uses three main steps:

1. Fitting a harmonic model
2. Detecting changes
3. Calculate change magnitude within the period of monitoring

In order to assess if a change in land cover occurs at pixel level, the time series is split in two: a history period and monitoring period. A regression model is fit on the observations during the history period. This regression model can be specified by the user, according to a priori knowledge of the study area. For e.g. in the case of evergreen

forests with limited seasonality, the regression model is a constant linear model (the mean of the observations), while in the case of deciduous forest with seasonality, the regression model is a first order harmonic function. The regression model can be applied to the whole history period (defined as starting from the first observation until the beginning of the monitoring period), or it can be applied only on a part of the history period that can be considered stable (starting from a defined moment until the beginning of the monitoring period). This moment that delineates a stable period in the history period can be provided by expert knowledge or can be calculated automatically using the reverse-order-cumulative sum (ROC or CUSUM) of residuals (Verbesselt et al., 2012b). This statistical algorithm moves backwards in time, from the starting moment of the monitoring period, and evaluates a cumulative prediction error until the season-trend model breaks down, defining the end of the stable history period. The stable history should be long and frequent enough to detect the changes in forest cover accurately (i.e. at least two years with an optimal temporal resolution of 16 days, as stated by Verbesselt et al., 2012b). It is also important that no limiting factors such as clouds or cloud shadows obstruct the satellite images indifferent of the period in which these occur (e.g. peak season of the tree growth).

As described by DeVries et al. (2015), to detect breakpoints in pixel time series, the moving sums (MOSUM) approach was used to monitor structural changes. This statistic approach checks if the newly acquired data in the monitoring period still fits the previously determined model. MOSUM applied on the residuals is a measure of discrepancy, having values close to 0 if the model remains stable, or systematically deviations from 0, in case a structural change occurs. A structural break is declared if the absolute value of the moving sum exceeds a 95% confidence interval of the calculated residuals in the history period (Verbesselt et al., 2012b). The magnitude is computed as the median of the difference between the data and the model prediction in the monitoring period.

3.2.2 BFAST Spatial

BFAST Spatial is a tool developed by L. Dutrieux, B. DeVries and J. Verbesselt (Introduction to bfastSpatial, 2016) that applies the pixel based approach of BFAST Monitor (described above) in a spatial context. As the authors state, by default, the output of BFAST Spatial is a three layer stack: (a) timing of breakpoints detected for each pixel (breakpoint); (b) the median of the residuals within the monitoring period (magnitude) and (c) a value for the pixels which were assigned an error by the algorithm (error) (Dutrieux et al., 2015; Dutrieux et al., 2016).

The magnitude is computed for each pixel regardless if a breakpoint is detected or not in the monitoring period. To detect deforestation, a structural change is expected, and so, only the magnitude for the pixels where a breakpoint occurred is going to be considered.

Considering only the presence or absence of breakpoints to define deforestation is not sufficient, as breakpoints associated with positive magnitudes or negative, but close to zero magnitudes, do not translate directly to deforestation. To avoid false positive deforestation detections, only breakpoints with a magnitude above a threshold should be considered (DeVries et al., 2015b). This threshold is dependent of the study area and calibrating of the magnitude threshold against reference data is an important step of the analysis.

14

3.3 Methodology diagram

In order to answer the research (RQ) and sub-research (SRQ) questions, the methodology presented in Figure 5 was followed. Every step is going to be detailed in the sections that follow the diagram below. The software used to conduct the analyses are presented in Appendix A.
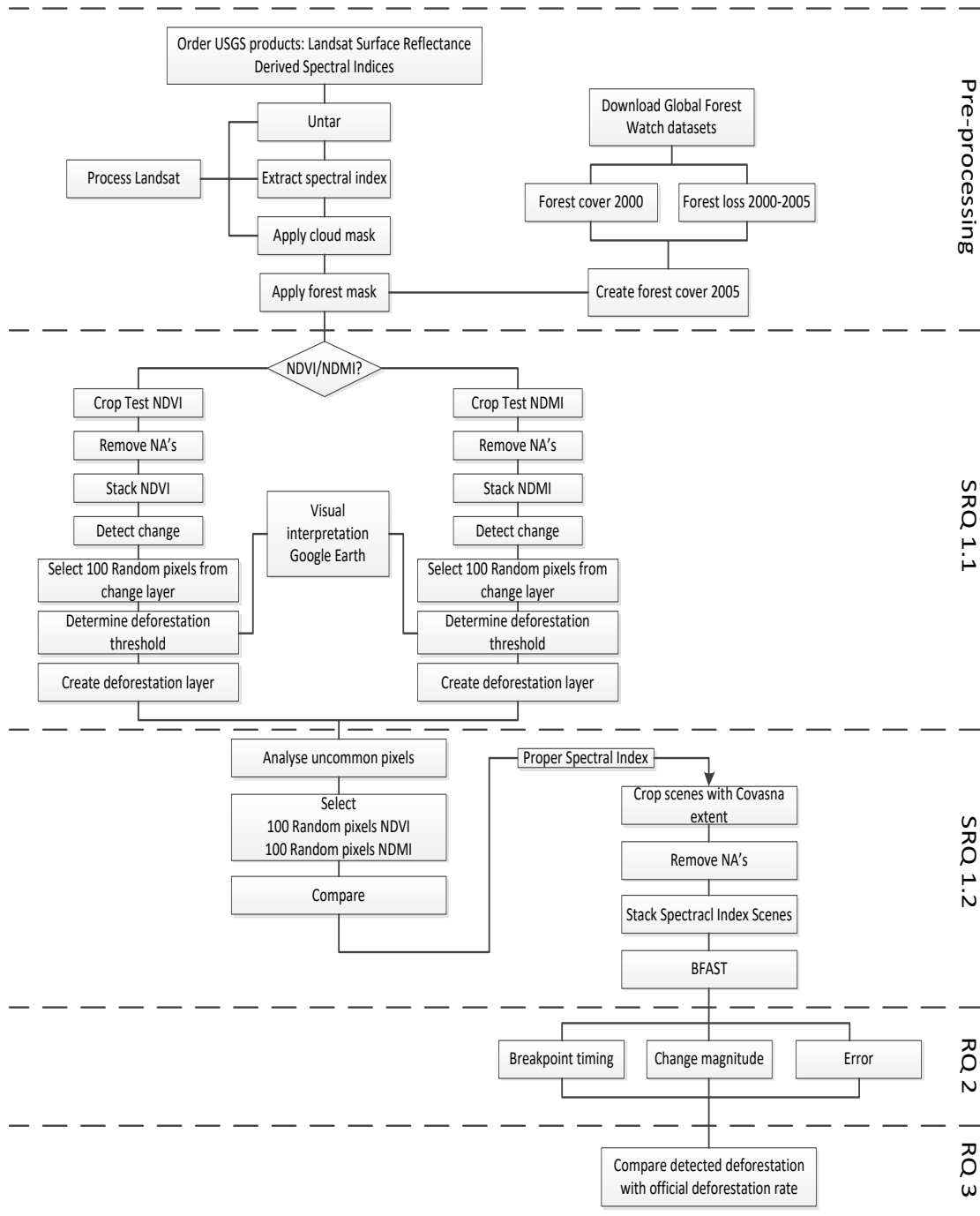
Figure 5. The pursued methodology diagram, which indicates the pre-processing steps, research (RQ) and sub-research (SRQ) questions

3.4 Data acquisition and pre-processing

The first step of the pre-processing section was to order the products from the USGS database (i.e. for both NDVI and NDMI), after which they have been extracted (i.e. from the .TAR archives). The next two steps were to apply the cloud and forest masks for each scene. These procedures are to be explained in the sections below.

3.4.1 Landsat products

For this study, all available Landsat 7 and 8 products corresponding to path 183, row 28 were freely downloaded from USGS database (.TAR file type) (Landsat USGS, 2016a). In total, at the time of the selection, 183 Landsat 7 scenes, and 55 Landsat 8 scenes were available from 14 February 2000 to 24 December 2015 (Figure 6), one scene covering entirely the area of interest (AOI). For the history period, there have been 39 satellite images used (i.e. only Landsat 7 images). The decision regarding the length of the monitoring and history periods was made such that both Landsat 7 and 8 scenes were used. The NDVI and NDMI derived from the surface reflectance product (see section 2.3.2 Surface reflectance) and individual cloud masks for each scene, were provided directly by the USGS.
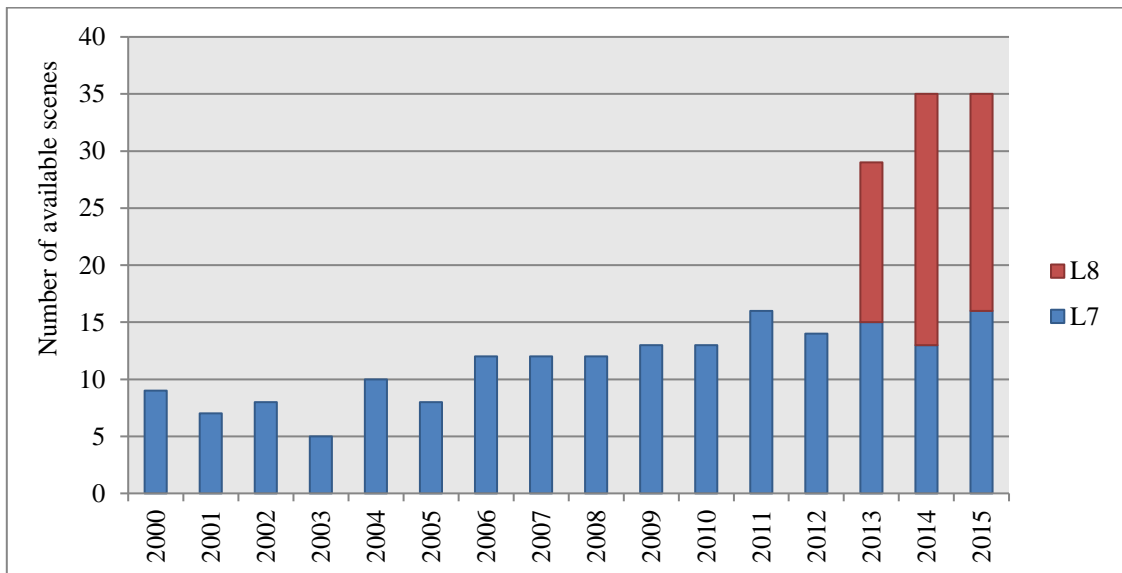
Figure 6. Landsat images (Landsat 7 in blue- 183 scenes and Landsat 8 in red- 55 scenes)– Chart that indicates the number of available scenes per year from 2000 (beginning of the history period) to 2015 (end of the monitoring period)

3.4.2 Cloud mask

Using RStudio (Version 0.99.879, RStudio Inc., Boston, United States) with "raster" package, the Landsat scenes along with Covasna County shape file extent were cropped, generating a new set of rasters. The same step was followed concerning the cloud masks for each NDVI and NDMI products. As illustrated in Figure 7, the following step was to use the Fmask products (i.e. cloud and cloud shadow; described in section 2.3.3 Clouds), in order to identify, select and remove the clouds from the scenes.

16
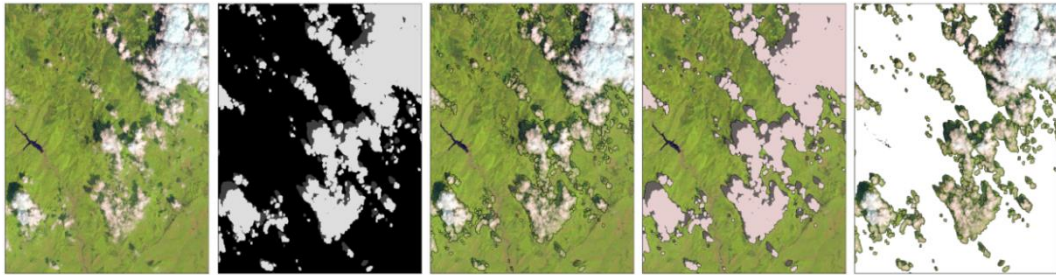
Figure 7. An example of cloud mask procedure (i.e. identifying, selecting and removing the clouds using the Fmask products for NDVI) for a small area in Covasna County

3.4.3 Forest mask

A forest mask has been applied to exclude non-forested areas from the study area and it was used later as a basis for the analyses. For this, rasters with forest cover from 2000 and forest loss from 2000 to 2015 were freely downloaded from the GFW database and later processed in order to determine the forest cover from 2005. To this end, the pixels, which represented the loss from 2000 to 2005 were selected and afterwards merged with the forest cover from 2000 (Figure 8). The new forest mask representing the forest cover in 2005 was therefore created. It represents the end of the history period which is considered undisturbed, as well as the beginning of the monitoring period. Since the GFW does not provide any yearly gain, but only the gain from 2000 to 2015, newly plantations have not been considered, the aim of this study being to detect only clear-cut deforestation on the area where there was forest in 2005. As scientific studies recommend (Baumann et al., 2012; Knorn et al., 2012), forested areas were defined as being pixels where the tree cover exceeds 60%. The GFW cover map has the same 30m x 30m spatial resolution as the Landsat imagery.
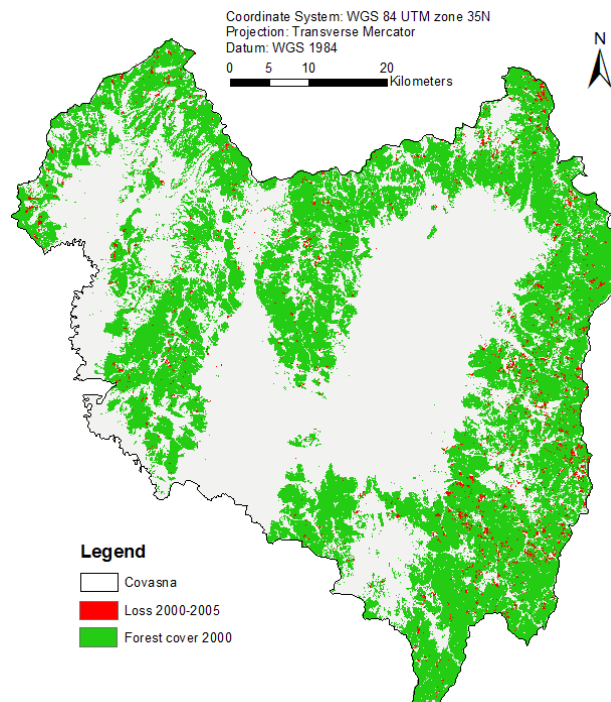
Figure 8. Map of forest cover in Covasna County in 2005 (Loss 2000-2005 in red, Forest cover 2000 in green and Covasna County border with black line)

3.5 RQ1. Detect clear-cut deforestation in Covasna, Romania, using BFAST

To answer to the SRQ 1.1 (i.e. How to translate change to detected clear-cut deforestation?) and SRQ 1.2 (i.e. What spectral index is most suitable to detect clear-cut deforestation?), the BFAST algorithm (which is explained in section 3.6.4 Applying BFAST) was used on a test area in order to determine the threshold and which of the NDVI and NDMI is the most suitable spectral index. The detailed procedures for these steps are presented in the following sections.

3.5.1 Test area

Directly applying the algorithm on the entire AOI could be inefficient when trying to decide what are the optimal parameters, therefore a smaller representative test area, has been chosen (Figure 9.) for this step. The test area was chosen based on GFW loss after 2005, a particular area where this indicates obvious deforestation. The decision regarding the parameters has been made based on the results obtained for this test area.
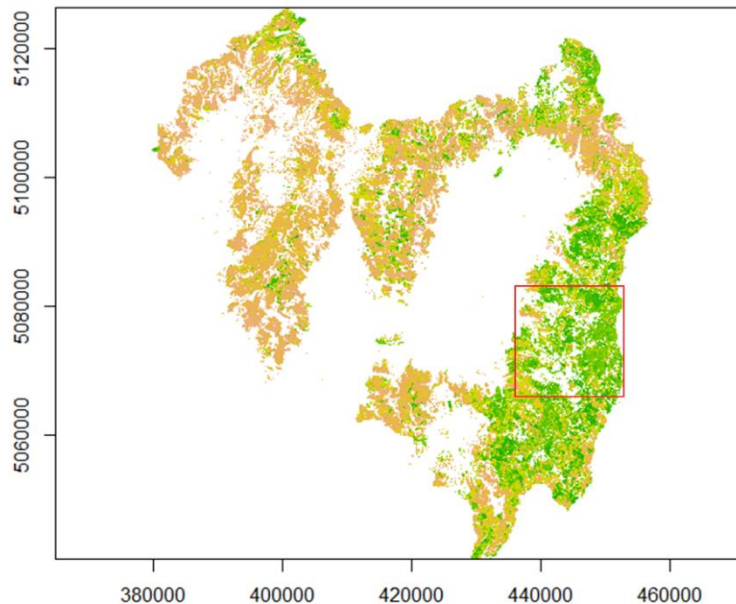
Figure 9. Map of forest cover in Covasna. The red rectangle indicates the selected test area and from brown to green are indicated the values of the NDVI product

3.5.2 Magnitude threshold

Only scenes that were not completely covered by clouds were considered for the analysis. Therefore, the scenes that contained just *not available* pixels (NA), after the Fmask procedure, were removed. After following the above steps, a time series stack was created using RStudio (Figure 11 in section 3.7.1 BFAST output layers), and afterwards the BFAST algorithm was applied for both NDVI and NDMI products individually.

As explained in chapter 3.2.2 BFAST Spatial, to determine which of the detected change is clear-cut deforestation (Figure 5, section SRQ 1.1- Detect change), a threshold for the magnitude of the change has to be determined. This threshold separates

18

clear-cut deforestation from other types of changes that can be detected in a forest (e.g. regrowth and degradation). Therefore, the deforested areas that had a threshold below the determined limit (see section 4.1.1 Threshold) were not considered to be clear-cut forest. The correct threshold for the magnitude layer was determined for each spectral index as illustrated in Figure 5 and detailed below.

To set the threshold value, 100 pixels were randomly selected for each NDVI and NDMI magnitude layers generated by the BFAST algorithm. For each of these random pixels, the visual interpretation was made using data from Google Earth (Version 7.1.2.2041, Google Inc., California, United States) (Figure 10), the threshold being selected using thresholding approach on these results. Since the most recent Google images analysed, for this test area, date from 2011, the 100 random pixels were chosen only from the pixels detected as deforested between 2005 and 2011. The interval selection process can be consulted in Appendix B.

Figure 10. Visual interpretation for NDMI magnitude threshold on a Google Earth image. The red squares represent the points where clear-cut deforestation was identified by the BFAST algorithm. The points coincide with the Google Earth deforested area.

After applying the BFAST algorithm, three layers have outcome (i.e. *change magnitude*, *breakpoint timing* and *error*), which are detailed in section 3.7.1 BFAST output layers. The *change magnitude* layer represents the deforestation layer.

3.5.3 NDVI vs. NDMI

To answer SRQ 1.2 (i.e. What spectral index is most suitable to detect clear-cut deforestation?; Figure 5, section SRQ 1.2), a deforestation layer was created using the resulting magnitude threshold for each index. From both NDVI and NDMI layers, 100 random pixels were selected from the pixels that were not commonly detected as deforested, in order to analyse which spectral index was more suitable for the AOI and this type of forest. A visual assessment has been made using Google Earth imagery and therefore, the most appropriate spectral index has been identified.

3.5.4 Applying BFAST

Knowing the most suitable spectral index, using RStudio, every scene was cropped with the Covasna shape, the NA have been eliminated (i.e. as in section 3.6.1 Test area), the time series was created and the BFAST algorithm was applied (Figure 5 Methodology diagram).

All the parameters of the algorithm (history period, monitoring period, as well as the formula for the regression model) were chosen based on the literature review (DeVries et al., 2016; Verbesselt et al., 2012a) as follows: (a) all the observations before 2005 were included in the history period instead of determining the stable history (ROC), due to the short length of this period, (b) the monitoring period was defined as the period after 2005, and (c) the harmonic order 1 was chosen as a regression model to fit the historical observations that were made on both coniferous and deciduous forests.

3.6 RQ2. Spatio-temporal distribution of clear-cut deforestation between 2005 and 2015

3.6.1 BFAST output layers

In order to answer RQ 2, but also to better understand how the algorithm works, and what are its inputs (i.e. *.TAR* archive ordered from USGS) and outputs, and how can the temporal parameter be included in the spatial data, the next diagram (Figure 11) has been followed:
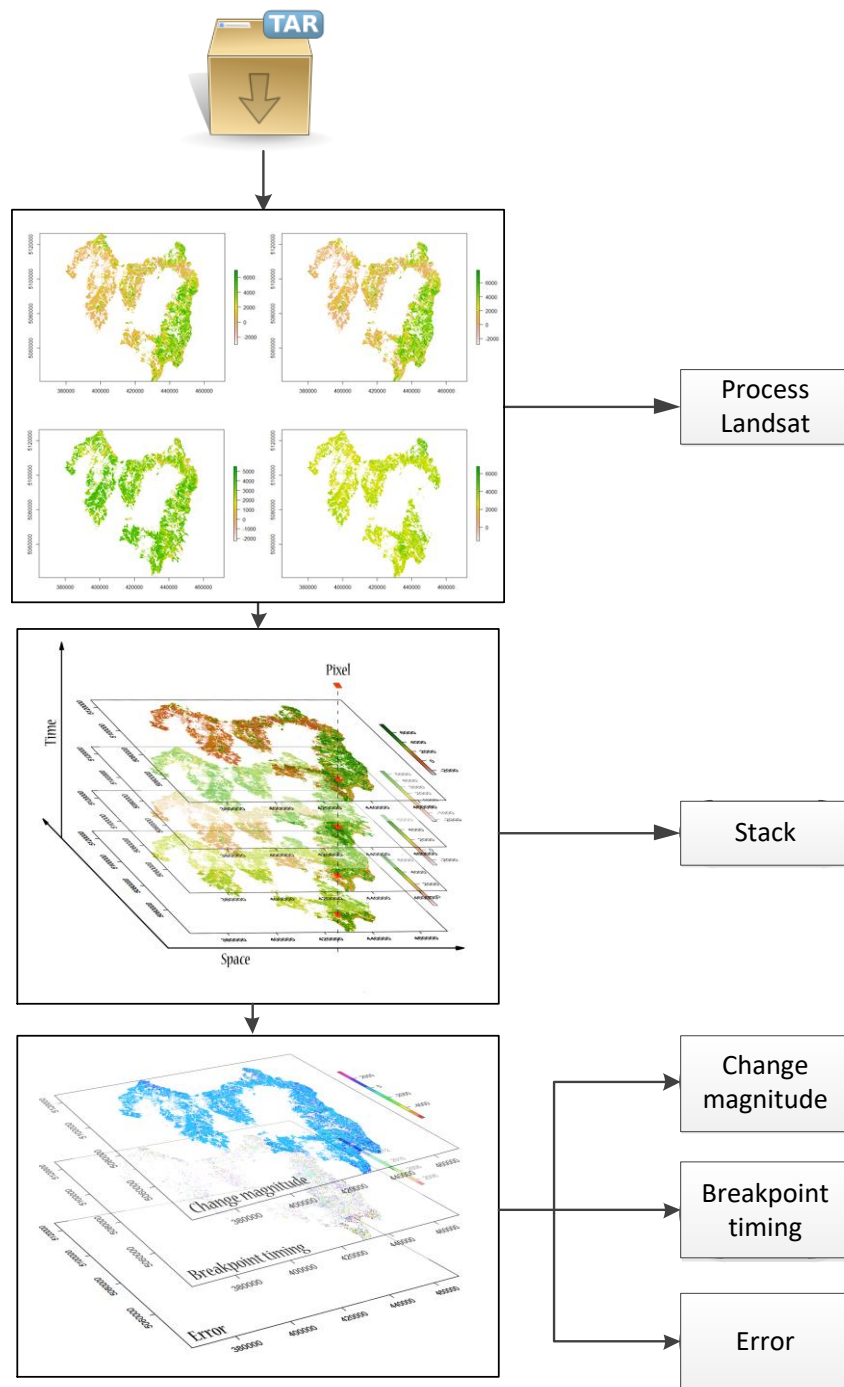
Figure 11. The pursued BFAST procedure (i.e. extracting the.TAR files, Landsat image processing (clouds mask and forest mask), stacking the resulted images, and the final results: change magnitude, breakpoint timing and error)

Three new layers resulted after applying the algorithm: *change magnitude*, *breakpoint timing* and *error*. In order to answer to RQ 2 (i.e. What is the spatio-temporal distribution of clear-cut deforestation between 2005 and 2015 in Covasna County, Romania?), *breakpoint timing* layer and *change magnitude* layer were analysed. Overlaying the *breakpoint timing* layer with the new *change magnitude* layer generated after setting the threshold has made it possible to analyse when clear-cut deforestation occurred during the monitoring period.

3.7 RQ3. Difference between the detected clear-cut deforestation and the official deforestation rate

To answer the last research question, RQ. 3, three data sets have been used (Figure 12): the total amount of clear-cut deforestation detected based on BFAST algorithm, the total amount of clear-cut deforestation provided by GFW and the National Institute of Statistics data sets (i.e. both clear-cut and selective). The latter provides the total cubic meters of exploited wood per year in Covasna County. The conversion from cubic meters to hectares will be explained in the results chapter.
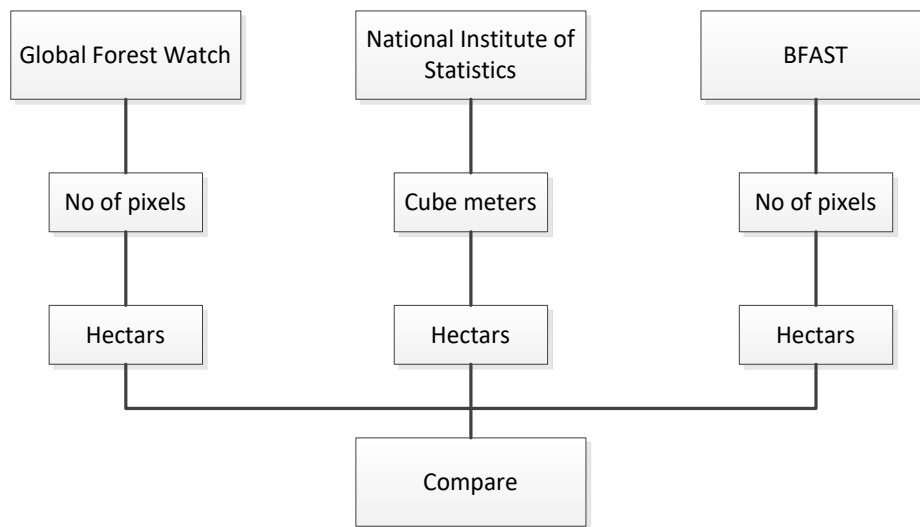
Figure 12. Comparison of deforestation between three datasets: GFW (from Global Forest Watch Database), National Institute of Statistics (National Institute of Statistics, 2016a) and the BFAST results. The conversion from number of pixels and cubic meters, respectively to hectares is detailed in chapter 4.2 RQ2. Spatio-temporal distribution of clear-cut deforestation between 2005 and 2015

A pixel from Landsat imagery measures 30 m on each side, meaning that each pixel measures 900 square meters or 0.09 ha.

Of course, a comparison between the National Institute of Statistics data and the BFAST detected clear-cut deforestation or GFW layer is not conclusive enough because it is difficult to follow selective logging. Thus, these two data sets will be discussed in comparison with the present study results in the Results chapter.

3.8 Validation

For interpreting forest cover change in Covasna County, Romania, only remote sensing data products were available, no "ground truth" data being used. Therefore, to validate the data and check the accuracy, a visual assessment has been done to indicate the reliability of the method. The visual interpretation has been performed on Google Earth images as they have higher spatial resolution than Landsat data, which has 30 meters resolution. First, due to the lack of recent Google Earth imagery for the whole study area, the results from a specific area situated towards the eastern part of the AOI were

excluded (Figure 13). Pixels that represented areas deforested later than 2014 (i.e. the Google Earth image used in the visual interpretation process) were also excluded.
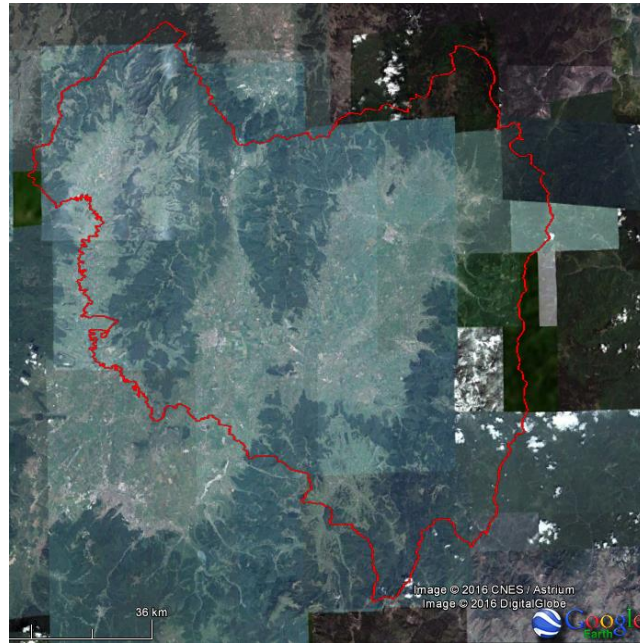
Figure 13. The image represents all the available Google Earth images for the study area (Covasna County, in red), the central-eastern and north-eastern part being excluded due to the lack of recent Google Earth imagery

As a result, 100 random pixels over the deforested area have been selected for the visual interpretation. From these pixels, those that have been correctly detected were assigned an *agree change* value and those which have not been properly detected were defined as a *commission* error.

For detecting the overall accuracy, another set of 100 random pixels had to be selected in the forested area. The forested area being much more widespread than the deforested area, selecting pixels from this particular area would not have been relevant. For this reason, pixels have been chosen from a one-pixel size width buffer, which was created around the edges of the clear-cut deforestation layer. Considering that not all the deforested areas are entirely surrounded by forest, the edges situated near other types of land use were also excluded from the buffer. An example of this situation will be presented in the results chapter. From the selected pixels, the ones that have been correctly detected were assigned an *agree no change* value and those which have not been properly detected were defined as an *omission* error.

4. Results

4.1 RQ1. Detect clear-cut deforestation in Covasna, Romania using BFAST

4.1.1 Threshold

As magnitude ranges for NDVI and NDMI differ, a threshold for each range was set. Considering that BFAST also detects breaks that have positive or minimal change magnitude values that do not reveal deforestation (i.e. degradation or regrowth), the threshold range was carefully set. On the test area, the NDVI changes vary between -1800 and -500, while for NDMI, the values vary between -1200 and -200. The method described in the methodology, regarding the selection of threshold applied on the test area for the random pixels, led to the following threshold values: -350 for NDVI and -850 for NDMI (see Appendix B). Therefore, SRQ 1.1 (i.e. How to translate change to detected clear-cut deforestation?) was answered.

The answer for SRQ 1.2 (i.e. What spectral index is most suitable to detect clear-cut deforestation?) resulted from comparing the deforested areas (change with appropriate threshold) detected using NDVI, with deforested areas detected using NDMI. The results conclude that out of 100 random pixels in the test area, 73 were correctly detected in which NDMI is concerned, while only 67 were correctly identified in the NDVI's case. This result reveals that the NDMI products are more suitable to use on the entire AOI.

By using a suitable spectral index, combined with a proper threshold, clear-cut deforestation has been detected on the entire AOI.

4.1.2 Break detection on individual pixels

An example of time series analysis for one specific pixel in the test area between 2000 and 2015, in which a break was detected in 2010 (Figure 14) will be further discussed.
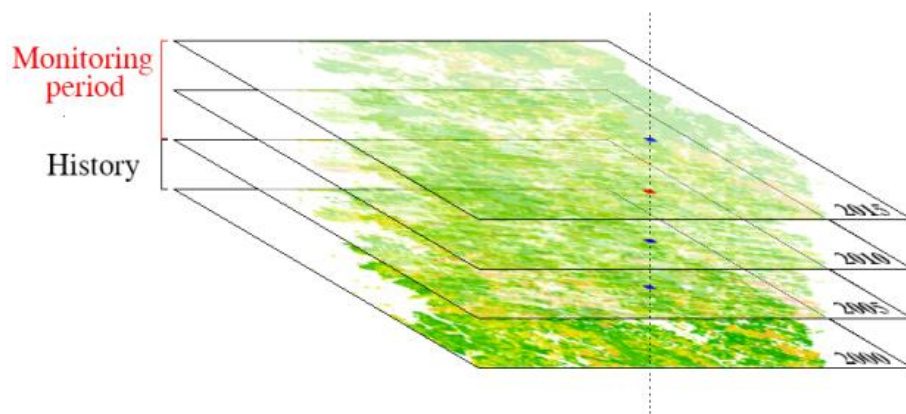
Figure 14. Pixel analysis – the detected break is indicated by the red point in 2010, the images representing the NDVI product from USGS database (the history period is considered from 2000 to 2005 and the monitoring period from 2005 to 2015)

The period between 2000 and 2005 is considered to be stable history. This interval is shown in Figure 15 on the left side of the black dotted line while the monitoring period

is displayed on the right side. The continuous black line represents the historical data while the blue line describes the prediction of the model, based on the historical data. The continuous red line represents new data from the monitoring period. A forest disturbance was detected on the 120th day of 2010 (i.e. the 30th of April) highlighted by the vertical red dotted line.

Figure 15. An example of pixel analysis from 2000 to 2015, where the black continuous line represents the historical data, the red continuous line represents the new data and the blue continuous line represents the prediction of the model. The vertical black dotted line represents the start of the monitoring period and the red dotted line represents the time of detection (2010)

In contrast with the above-presented break detection, Figure 16. Pixel analysis – The blue points indicates that there is no break detected and Figure 17 displays a case in which no break was detected, as the prediction of the model is approximately coinciding with the new data from the monitoring period.
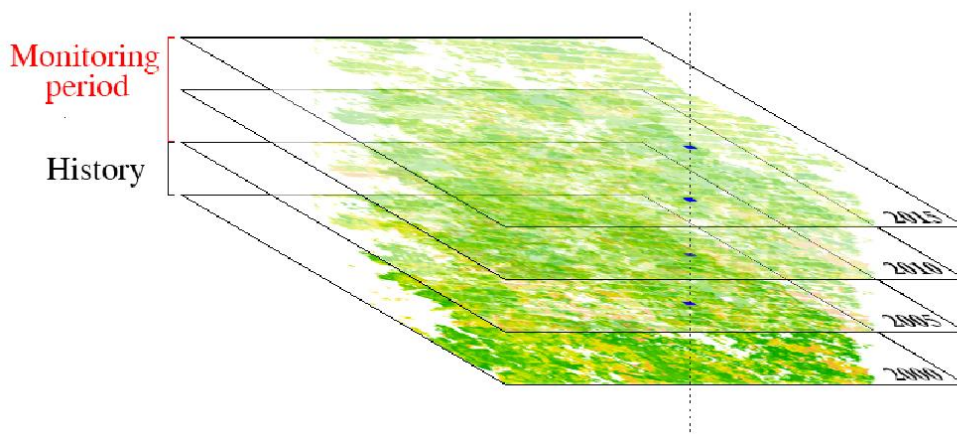
Figure 16. Pixel analysis – The blue points indicates that there is no break detected. The images represent the NDVI products from USGS database (the history period is considered from 2000 to 2005 and the monitoring period from 2005 to 2015)
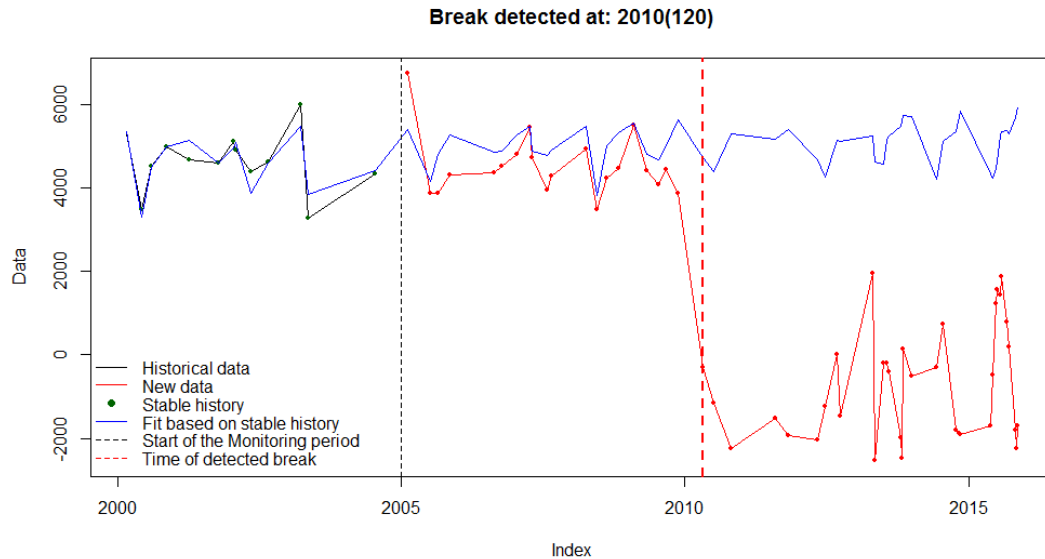
25

No break detected

Figure 17. An example of pixel analysis from 2000 to 2015 (no break detected), where the black continuous line represents the historical data, the red continuous line represents the new data, the blue continuous line represents the prediction of the model. The vertical black dotted line represents the start of the monitoring period. In this case, the new data (red line) almost coincides with the predicted data (blue line)

4.2 RQ2. Spatio-temporal distribution of clear-cut deforestation between 2005 and 2015

4.2.1 Temporal distribution

In order to compare the total surface of deforested areas and determine the general trend throughout the monitoring period, three different data sets have been used: Romanian Court of Audit dataset, loss of forested areas provided by GFW and the BFAST results. The three distinct data sets have different measure units. Therefore, the data has been converted into hectares in all three cases.

It is important to mention that the data from the National Institute of Statistics which include both clear-cut and selective deforestation were provided only in cubic meters. Therefore, the conversion was possible by using the information provided by the Romanian Court of Audit which states that the mean volume of wood on one hectare is 218 m^3 (Curtea de Conturi, 2014). It is stated that generally, the ratio between the coniferous and deciduous trees within a forest in Romania is of 35 and 65, respectively. In Covasna, the ratio of tree species composition is similar to the previously mentioned ratio (i.e. entire country). Therefore, the mean volume of wood on one hectare (i.e. 218 m^3) was used for this study. The conversion from cubic meters to hectares is presented in Table 1 below, the general trend of deforestation being illustrated in Figure 18.

Table 1. The conversion from cubic meters of declared deforestation per year for Covasna County to hectares from 2005 to 2014 (National Institute of Statistics, 2016b)

Year	Year 2005	Year 2006	Year 2007	Year 2008	Year 2009	Year 2010	Year 2011	Year 2012	Year 2013	Year 2014	Total
Covasna x10³ m³	545.5	462.8	485.4	443.6	495.7	511.6	545.3	576.4	626.2	632.9	4692.5
Hectares	2502	2122	2226	2034	2273	2346	2501	2644	2872	2903	21525
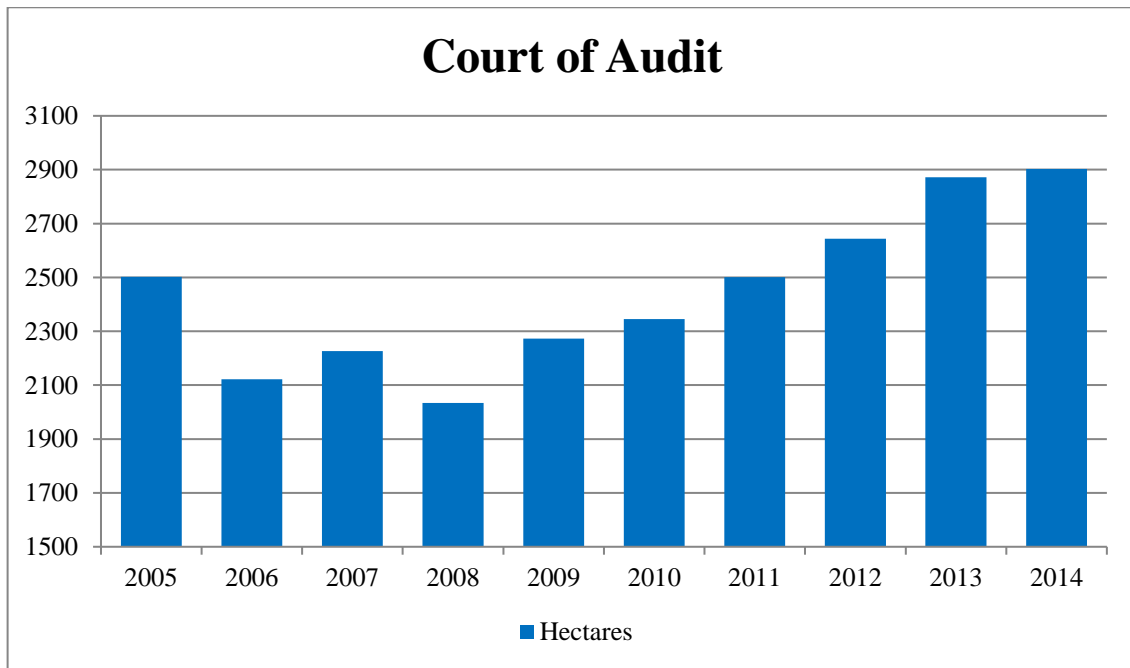
Figure 18. Chart representing the total amount of deforestation (hectares per year) from the 2005-2014 time period, declared by the Court of Audit. The lowest amount of deforestation was declared in 2008, while the highest amount was declared in 2014

Concerning the GFW data, knowing that one pixel measures 0.09 ha, the information has been transformed from pixels to hectares as shown in the following table (Table 2).

Table 2. The conversion from number of pixels (i.e. one pixel measures 0.09 ha) per year (GFW) to hectares from the 2005-2014 time period

Year	Year 2005	Year 2006	Year 2007	Year 2008	Year 2009	Year 2010	Year 2011	Year 2012	Year 2013	Year 2014	Total
Number of pixels	5754	5063	3693	5830	3511	3478	5435	5582	4496	5081	47923
Hectares	517.9	455.7	332.4	524.7	316.0	313.0	489.2	502.4	404.6	457.3	4313.1

Similarly, the temporal distribution of the clear-cut deforestation resulted from BFAST algorithm is presented in Table 3, below.

Table 3. The conversion from number of pixels per year (BFAST results) to hectares from the 2005-2015 time period

Year	2005	2006	2007	2008	2009	2010	2011	2012	2013	2014	2015	Total
Number of pixels	3103	3356	5249	4069	3361	2874	2782	1776	5183	793	262	32808
Hectares	279	302	472	366	302	259	250	160	466	71	24	2953

The highest amount of clear-cut deforestation is recorded in 2007 and 2013.

4.2.2 Spatial distribution

Romania's territory is divided in Counties, and the Counties in Territorial Administrative Units (TAUs). Covasna County has 43 TAU's, information about the spatial distribution of deforested areas from 12 of the most relevant TAUs being presented in Table 4, the rest of the territory (31 TAUs) summing a number of 5794 pixels (i.e. 521.5 hectares). The map which indicates the clear-cut deforestation detected in Covasna County can be consulted in Appendix C.

Table 4. The conversion from number of pixels representing deforested areas to hectares for the most affected TAUs in Covasna County from BFAST results. The highest amount of deforestation is situated in Zagon, Covasna and Ghelinţa TAUs

Locality	Brăduţ	Breţcu	Comandău	Estelnic	Ghelinţa	Mereni	Ojdula	Covasna	Sînzieni	Sita Buzăului	Zăbala	Zagon
No of pixels	713	783	922	3165	4726	858	1564	3682	923	578	1734	7944
Hectares	64	70	83	285	425	77	141	331	83	52	156	715

28

Figure 19 highlights the 3 most affected TAUs in Covasna County: Ghelinţa, Covasna (the TAU has the same naming as the County) and Zagon (Figure 20).
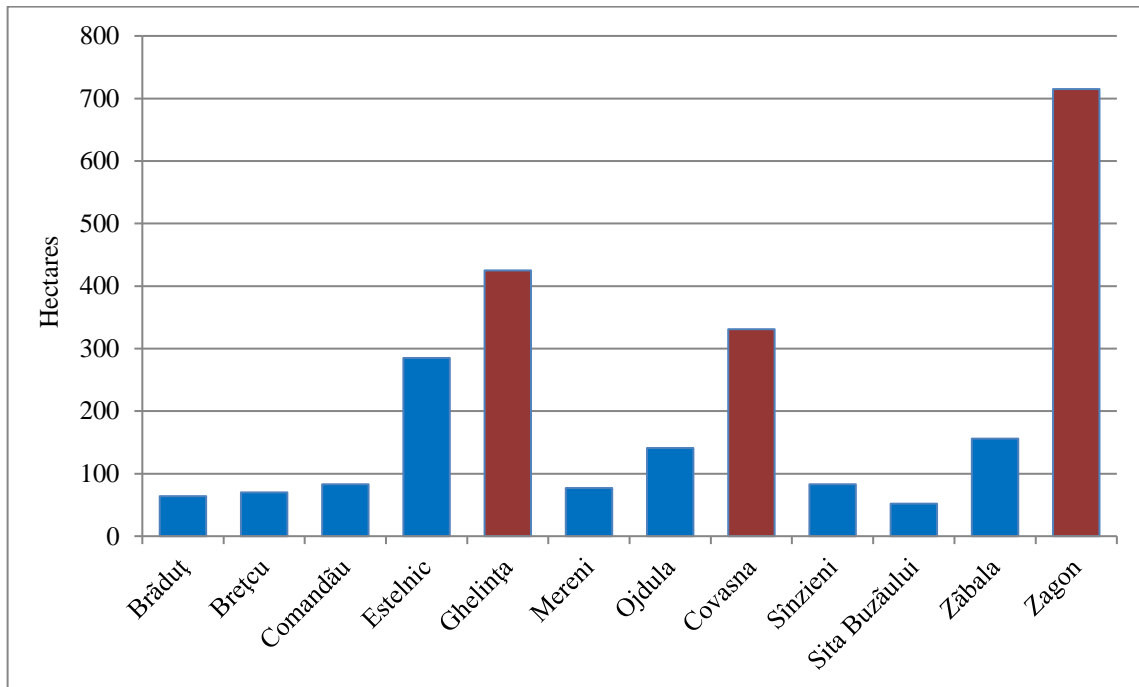
Figure 19. Chart indicating the most affected TAUs from Covasna County by clear-cut deforestation (hectares per TAUs). In red are highlighted the highest amounts of clear-cut deforestation (Ghelinţa, Covasna and Zagon)
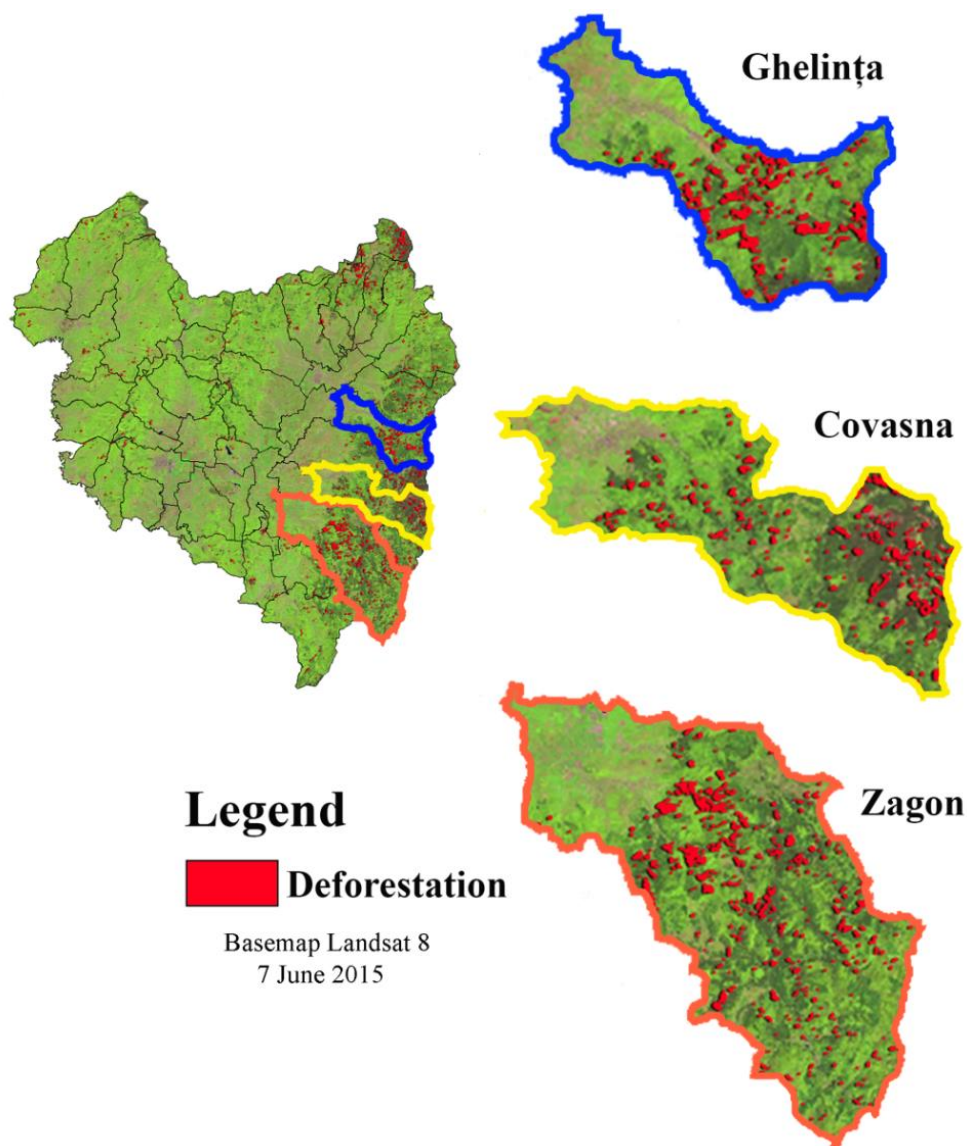
Figure 20. Clear-cut deforestation (BFAST results) in Ghelința (blue), Covasna (yellow) and Zagon (red) TAUs, which are the three most affected TAUs in Covasna County. The basemap is a Landsat 8 image from 7 June 2015

4.3 RQ3. Difference between the detected clear-cut deforestation and the official deforestation rate

4.3.1 Comparison between results

As described in Figure 21, a comparison between the Court of Audit, GFW and BFAST sets of values has been conducted. This comparison helps to a better understanding of the ratio between the present study results regarding clear-cut deforestation and the total deforestation amount (i.e. clear-cut and selective deforestation), as declared by the Court of Audit. From this comparison, it results that the clear-cut deforestation represents approximately 15% of the total deforestation (i.e. clear-cut and selective deforestation) (Court of Audit) for almost all years of the monitoring period.

30
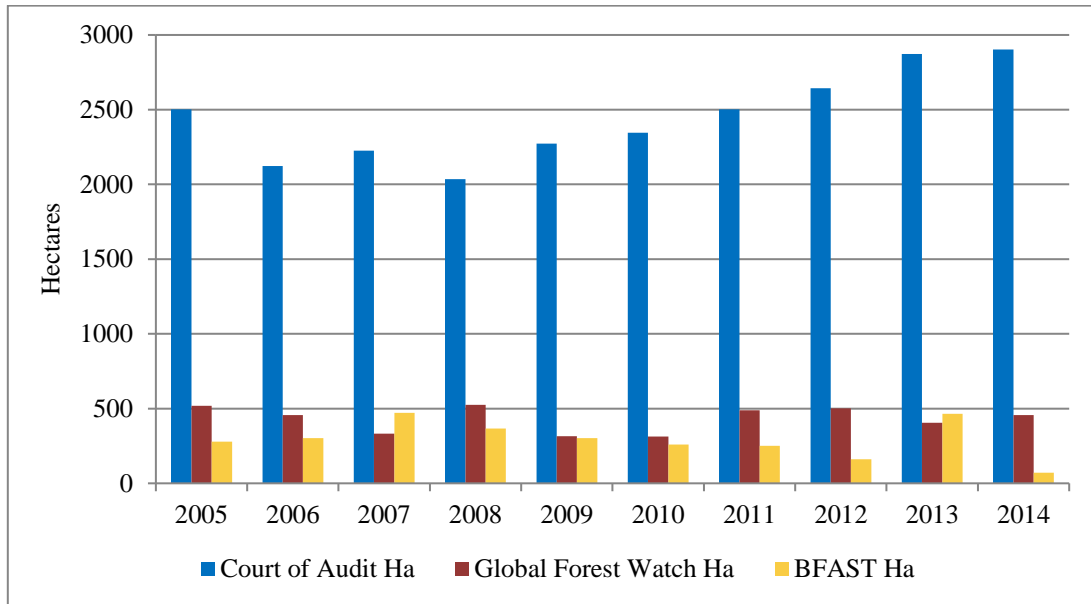
Figure 21. Chart representing the total amount of deforestation (blue - Court of Audit) and clear-cut deforestation (red - GFW and yellow - BFAST)

4.3.2 Clear-cut deforestation rate

The yearly clear-cut deforestation rates were determined based on the results in Table 3, for each year of the monitoring period. The rates are presented in Table 5. These results indicate that clear-cut deforestation has decreased from 2007 onwards, but for year 2013.

Table 5. Clear-cut deforestation rate (The rates indicate that clear-cut deforestation has decreased from 2007 to 2015)

Year	2005	2006	2007	2008	2009	2010	2011	2012	2013	2014	2015	Total
Hectares	279	302	472	366	302	259	250	160	466	71	24	2953
Rate	0.16	0.17	0.27	0.21	0.17	0.15	0.14	0.09	0.27	0.04	0.01	1.71

4.4 Accuracy assessment

As introduced in the methodology, in order to validate the resulted data, two sets of random pixels have been selected from the deforested, respectively forested areas. Thus, a buffer was created in order to select the second set of random points. An example of the previously described procedure is illustrated in the following figure.
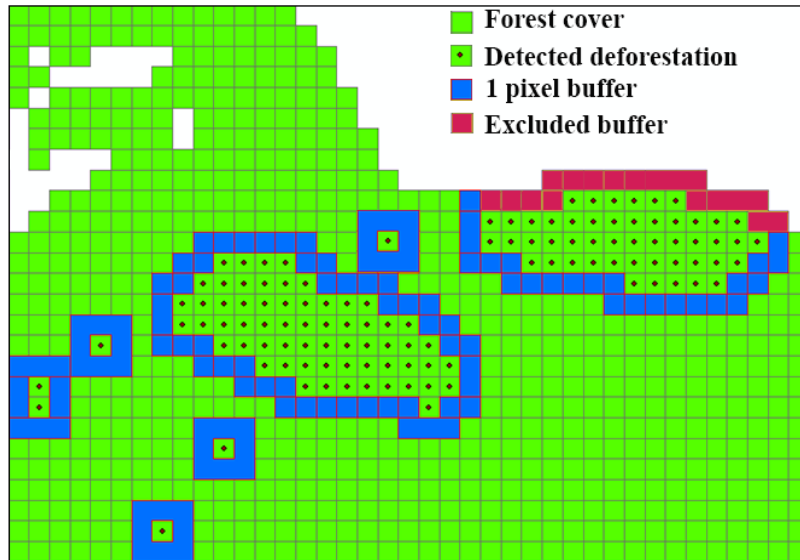
Figure 22. An example of buffer created to select random points from the forested area in order to check the accuracy (forest cover – green squares, detected deforestation – green squares with dots, 1 pixel buffer – blue square and excluded buffer – red square)

Figure 22 describes the status of each visually interpreted pixel. Accordingly, the correctly detected pixels from the randomly selected deforested area were considered as *agree change*, while the incorrectly detected pixels were considered *commission* errors. Regarding the second set of points, the correctly determined pixels were declared as *agree no change*, while the rest were considered *omission* errors. The spatial position of the random points is presented in Figure 23, below.

32
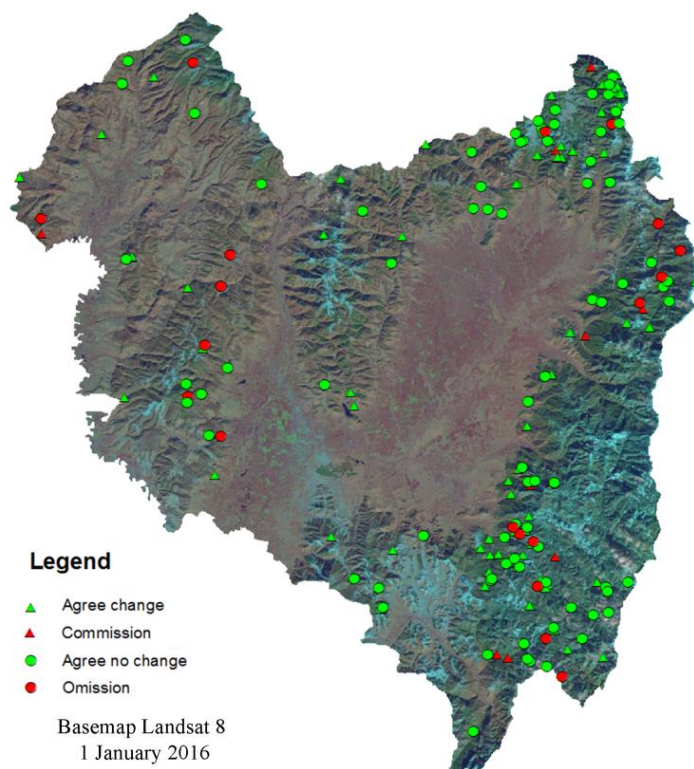
Figure 23. Random pixels (i.e. 200) selected to determine the accuracy (*agree change* – green triangle, *commission* – red triangle, *agree no change* – green circle and *omission* – red circle). The basemap is a Landsat 8 image from 1 January 2016

Based on the previously described validation results, an error matrix has been determined in order to check the overall accuracy. The overall accuracy concerning the two land cover classes (i.e. deforested and forested areas) resulted in a value of 84%, which concludes on the adequacy of the algorithm for the present study. The results of the visual interpretation and consequently the error matrix are shown in Table 6.

Table 6. Error matrix used to check the overall accuracy (actual and predicted classes). The overall accuracy resulted in a value of 84%

<table>
<tr><td rowspan="6">Actual class</td><td colspan="4" align="center">Predicted class</td></tr>
<tr><td></td><td>Deforested</td><td>Forested</td><td>Total</td></tr>
<tr><td>Deforested</td><td>87</td><td>13</td><td>100</td></tr>
<tr><td>Forested</td><td>19</td><td>81</td><td>100</td></tr>
<tr><td>Total</td><td>106</td><td>94</td><td>100
100</td></tr>
</table>

5. Discussion

5.1 Detecting clear-cut deforestation with BFAST

As presented in the Literature Review chapter, the BFAST algorithm was successfully used in various locations with different types of forest.

In their studies, Schultz et al., 2015, DeVries et al., (2015), Hamunyela et al., 2016 and Decuyper et al., 2015 used the BFAST algorithm on wet evergreen natural forest (Vietnam), moist broadleaf evergreen forest (Kafa Biosphere Reserve, Ethiopia), on evergreen tropical forest (Ariquemes, Rondonia State, Brazil), and tropical forests in Madre de Dios (Peru) and Para (Brazil), respectively. In contrast, Watts and Laffan, 2014 and Tsutsumida et al., 2013, used the algorithm on a semi-arid area in Queensland (Australia) and an urban area in Ulaanbaatar (Mongolia). Lambert et al., 2013 used the algorithm in Massif Central Mountains (France) on coniferous forest and Hutchinson et al., 2015 uses the algorithm to detect disturbance created by fire on grassland in Fort Riley (Kansas, United States of America). In relation to the previously mentioned studies, the results on the temperate forest (which is composed mostly on deciduous and coniferous) of the present study indicate that the algorithm is flexible and adaptable. The adaptability of the algorithm to different types of land use is highlighted by its successful results from the coniferous forest in France to the semi-arid area in Australia and urban area in Mongolia.

Applying the BFAST algorithm to detect clear-cut deforestation is not as data-driven as the authors imply it is, since multiple settings have to be thought beforehand and they differ from area to area. Decisions have to be made regarding the history period, the regression function to fit the stable observations, and a threshold has to be determined to define change as clear-cut deforestation.

In this respect, a longer historical data interval will fit better the stable history period, which will finally lead to better accuracy. If there is apriori knowledge that a deforestation event followed by a regrowth period occurred in the history period, which is supposed to represent observations of stable forest, then the history period has to be changed accordingly either manually or by using the ROC approach when applying BFAST. The present study highlighted that lower NDVI/NDMI magnitude thresholds will led to an enhancement in the commission error while higher threshold values will result in enhanced omission error. Moreover, calibrating the threshold on visually interpreted reference data, has implications in the repeatability this study or for reproducing this method in other similar study areas. Therefore, instead of using Google Earth images for the visual interpretation process, it is recommended that field data be collected.

Considering that Covasna is covered by both coniferous and deciduous forest, the present method could be successfully extrapolated to country level.

Regarding the comparison between BFAST results and the forest loss provided by GFW, there are a few differences, of which the use of Landsat 5 imagery in the GFW data, which could improve the results (i.e. Landsat 5 satellite has the same temporal resolution as Landsat 7 and 8, but different crossing time over a specific area). It is important to mention that both BFAST results and forest loss provided by GFW do not include any forest degradation, as stated in section 2.3.5 Global Forest Watch.

5.2 Clear-cut deforestation in Covasna County, Romania

As highlighted in the Results chapter, clear-cut deforestation is a present-day issue in Covasna County. However, the decrease detected from 2008 (Table 5) onwards could be due to the law no. 46 art.51, which was adopted on the 19th of March 2008 and states as the private owners of the forest are responsible for the security of their property regarding illegal logging, destruction, degradation and grazing (Law 46/2008).

Since a national forest inventory in Romania occurs only every five years, verifying the legitimacy of the deforestation could be difficult considering the large time span. Using the tool introduced in the present study, which detects clear-cut deforestation in near real-time and can produce one-year temporal resolution clear-cut deforestation maps, could be useful in order to verify the legitimacy of deforestation regarding clear-cut logging.

5.3 Month discussion

An interesting correlation might exist between cloud cover and the months when clear-cut deforestation has been detected. As highlighted in Figure 25, the cloud cover percentage suddenly decreases in April, due to the beginning of the warm season. Consequently, even if clear-cut deforestation would occur in one of the cold season months, it will not be observed from the satellite images until April, due to cloud covering. The peak in Figure 24, along with April cloud cover values (Figure 25), show that these two sets of values might be interconnected. Likewise, the low cloud cover values in November, which follow the rainy season (September-October), are also connected to the high values of monthly clear-cut deforestation. In contrast, months with high cloud cover values are associated with low detected clear-cut deforestation values. Therefore, the detected monthly clear-cut deforestation rate appears to be influenced by the cloud cover percentage of each month. This impedes the determining of the temporal accuracy. Also, when working with time series, it is important that relevant images be as frequent as possible, as stated in section 3.3.1 BFAST Monitor. This is the reason why all images, indifferent of their cloud cover percentage, were used in this study.
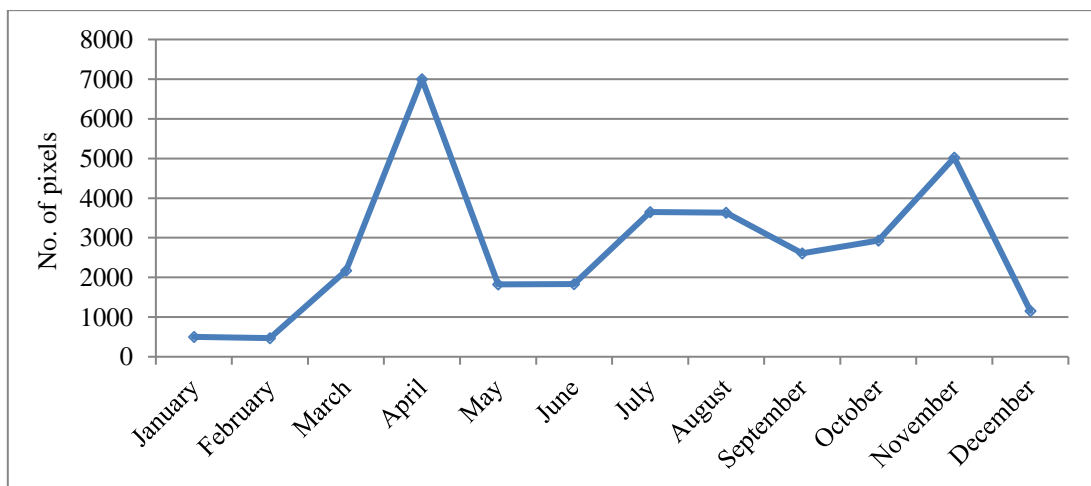
Figure 24. Chart representing the total clear-cut deforestation (all years from the monitoring period) per month, the highest values of monthly clear-cut deforestation being detected in April and December
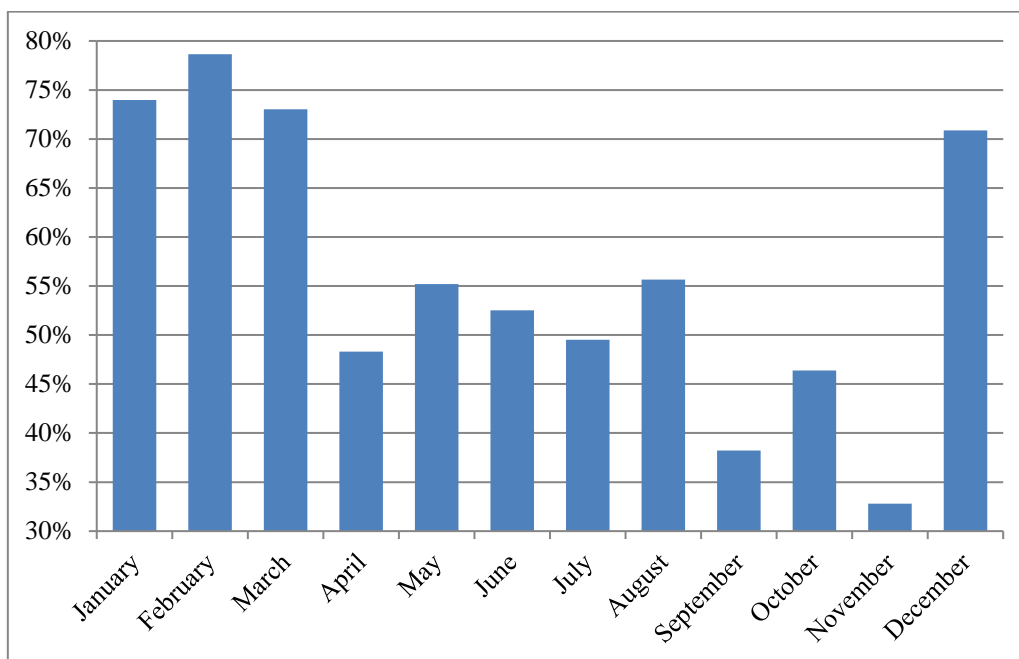
Figure 25. Chart representing the mean of cloud cover per month. All the images from the monitoring period and the Fmask products were used to determine the percent of cloud cover. As the chart highlights, late winter and beginning of the spring are the cloudiest period during a year

5.4 Accuracy comparison

The overall accuracy determined by the present study has a value of 84%, which is a rather satisfying result, considering the total surface of the AOI and the type of forest. This result shows that the BFAST algorithm is suitable in order to detect clear-cut deforestation in Romania (i.e. both coniferous and deciduous forest in a temperate climate). In order to confirm this result, below are presented a few examples of similar accuracies that have been obtained in other studies (Table 7).

Table 7. Accuracy comparison of BFAST algorithm between different scientific studies (the table indicates the author, the forest type, the location and the overall accuracy of each study)

Author	Forest type	Location	Accuracy
Schultz et al., 2015	Tropical	Brazil	79.4%
		Ethiopia	60.5%
		Vietnam	82.2%
Dutrieux et al., 2015	Tropical dry	Bolivia	87%
Lambert et al., 2015	Coniferous	France	82%
Reiche et al., 2015a	Evergreen	Fiji	87.4%
Decuyper et al., 2015	Tropical	Peru and Brazil	85%

5.5 Risk

According to the illegally harvested wood risk map of Romania (WWF, 2016), Covasna is not in the top of the illegal deforestation high-risk category, recording a percentage of 42%. It is important to emphasize that Figure 26 and the values from Table 8 do not indicate illegally deforested areas, but areas that are predisposed to this vulnerability. The data regarding the risk of illegally harvested wood was acquired from *World Wide Fund for Nature (WWF)* organization. The map was created based on multiple indicators (e.g. the volume of illegal logging in relation to the regular harvesting volume, the surface of the unsupervised forested area and the number of penalties reported to the administrative area). This map was created to increase the security in the vulnerable areas.
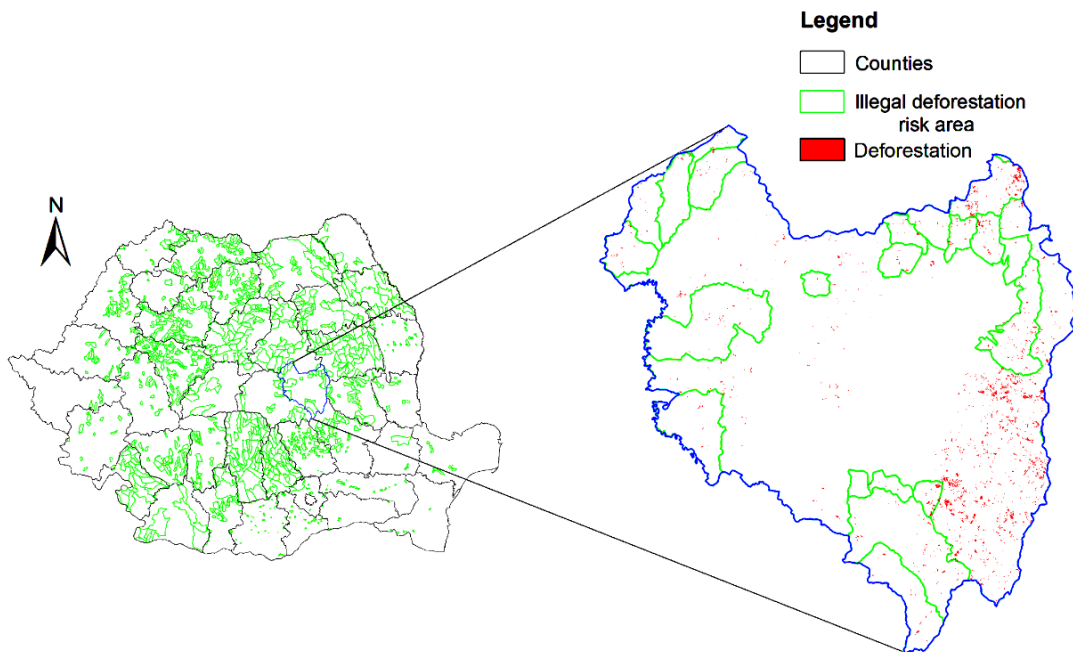
Figure 26. Map representing the illegal deforestation risk areas. The green line represents the illegal deforestation risk areas, the black line represents the counties, the red areas represent the deforestation (BFAST results) and the blue line indicates the boundaries of Covasna County (WWF, 2016)

Table 8. The areas with the highest illegal deforestation risk rate in Romania (WWF, 2016)

	County	Risk area red code	Risk area yellow code	Total risk area
1	Dâmbovița	72%	12%	84%
2	Argeș	67%	4%	71%
3	Bacău	53%	4%	58%
4	Olt	55%	0%	55%
5	Mehedinți	54%	0%	54%
6	Covasna	28%	14%	42%
7	Iași	33%	9%	42%
8	Alba	15%	27%	42%
9	Maramureș	36%	2%	38%
10	Buzău	35%	3%	38%

5.6 Recommendations for future research

A possible improvement for future research could be to differentiate between coniferous (i.e. evergreen with limited seasonality) and deciduous (i.e. with seasonality) forest, and to apply the algorithm on each forest type. Furthermore, as mentioned earlier in section 5.1. Detecting clear-cut deforestation with BFAST, it is expected that more satellite images will be available for further studies, which means that the history period would include more data and therefore it will be more stable. Consequently, this would conduct to better and more accurate results.

The commission error could be reduced if the detected isolated pixels are statistically checked for significance through random sampling and visual assessment.

6. Conclusions

Deforestation is still an ongoing process in which temperate forest is concerned, this issue being noticeable in Covasna County, Romania. The results of this study show a decrease in forest area of about 1.71% from 2005 to present. Considering the purpose of the study, the type of forest and the scale of AOI, the algorithm can be successfully used to detect clear-cut deforestation.

Choosing a magnitude threshold range could be problematic as a higher value would conduct to commission error while a lower value would result in omission error. The threshold used in the present study led to an overall accuracy of 84% regarding the chosen index (NDMI).

From the comparison between total deforestation amount declared by the Court of Audit with the clear-cut deforestation determined in the present study, results that the clear-cut deforestation represents approximately 15% of the total deforestation, which includes both clear-cut and selective deforestation (Court of Audit) for almost all years of the monitoring period.

Contrary to the official deforestation rate, that mainly shows an increase of the deforestation rate for the last 10 years, the results of this study present a decrease in clear-cut deforestation between 2005 and 2015.

References

Bartha, S.G., Quave, C.L., Balogh, L., Papp, N., 2015. Ethnoveterinary practices of Covasna County, Transylvania, Romania. J. Ethnobiol. Ethnomed. 11, 35.

Baumann, M., Ozdogan, M., Kuemmerle, T., Wendland, K.J., Esipova, E., Radeloff, V.C., 2012. Using the Landsat record to detect forest-cover changes during and after the collapse of the Soviet Union in the temperate zone of European Russia 124, 174–184.

Cai, S., Liu, D., 2015. Detecting change dates from dense satellite time series using a sub-annual change detection algorithm. Remote Sens. 7, 8705–8727.

Chen, X.C., Steinhaeuser, K., Boriah, S., Chatterjee, S., Kumar, V., 2012. Contextual Time Series Change Detection. Sdm 2013 503–511.

Chertov, O., Frank, G., Köhl, M., Schuck, A., Sjöberg, K., Standovár, T., Brusselen, J. Van, 2006. European Forest Types. Categories and types for sustainable forest management reporting and policy, Publication: Forest@ - Rivista di Selvicoltura ed Ecologia Forestale, Luxembourg: Office for Official Publications of the European Communities, 2006. Copenhagen.

Curtea de Conturi, 2014. Raport de audit al performanței modului de administrare a fondului forestier național în perioada 2010-2013 (Court of Auditors), București. Bucharest.

Davis, C., Petersen, R., 2016. Tools for Monitoring Global Deforestation, Reference Module in Earth Systems and Environmental Sciences. Elsevier Inc., Washington, DC, USA.

Decuyper, M., DeVries, B., Verbesselt, J., Joseph, S., Martius, C., Herold, M., 2015. A robust method for monitoring net forest disturbances in two South American sites with different data density. In: 8th International Workshop on the Analysis of Multitemporal Remote Sensing Images. pp. 5–9.

Deter, 2016. Coordenação-Geral de Observação da Terra - Projetos. URL http://www.obt.inpe.br/deter/ (accessed 4.8.16).

DeVries, B., Pratihast, A.K., Verbesselt, J., Kooistra, L., Herold, M., 2016. Characterizing Forest Change Using Community-Based Monitoring Data and Landsat Time Series. PLoS One 11, 121–147.

DeVries, B., Verbesselt, J., Kooistra, L., Herold, M., 2015a. Detecting Tropical Deforestation and Degradation Using Landsat Time Series. In: IGARSS 2014 / 35th Canadian Symposium on Remote Sensing, 2014-07-13/2014-07-18.

DeVries, B., Verbesselt, J., Kooistra, L., Herold, M., 2015b. Robust monitoring of small-scale forest disturbances in a tropical montane forest using Landsat time series. Remote Sens. Environ. 161, 107–121.

DIGI 24, 2015. Klaus Iohannis: Defrișările ilegale, un atac la siguranța națională . URL http://www.digi24.ro/Stiri/Digi24/Actualitate/Stiri/Klaus+Iohannis+Defrisarile+ile gale+un+atac+la+siguranta+national (accessed 4.8.16).

Dutrieux, L.P., Verbesselt, J., Kooistra, L., Herold, M., 2015. Monitoring forest cover loss using multiple data streams, a case study of a tropical dry forest in Bolivia. ISPRS J. Photogramm. Remote Sens. 107, 112–125.

Dutrieux, L.P.L., Jakovac, C.C., Latifah, S.H., Kooistra, L., 2016. Reconstructing land use history from Landsat time-series. Int. J. Appl. Earth Obs. Geoinf. 47, 112–124.

EU Natura 2000, 2016. Natura 2000 - Environment - European Commission . URL http://ec.europa.eu/environment/nature/natura2000/index_en.htm (accessed 3.22.16).

Food and Agriculture Organization of the United Nations, 2016. National Forest Monitoring Systems: Monitoring and Measurement, Reporting and Verification (M & MRV) in the context of REDD+ Activities. UN-REDD Programme . URL http://www.fao.org/3/a-bc395e.pdf (accessed 5.11.16).

Global Britannica, 2016. Covasna County, Romania . URL http://global.britannica.com/place/Covasna (accessed 3.21.16).

Grebner, D.L., Bettinger, P., Siry, J.P., 2013. Forest Regions of the World, Introduction to Forestry and Natural Resources, 21-76.

Green Report, 2016. Românii pot semnala orice tăiere de pădure prin aplicația „Harta tăierilor de păduri" | Green Report . URL http://www.green-report.ro/romanii-pot-semnala-orice-taiere-de-padure-prin-aplicatia-harta-taierilor-de-paduri/ (accessed 3.19.16).

Greenpeace, 2016. Pădurile din România au nevoie de voluntari . URL http://www.greenpeace.org/romania/ro/campanii/paduri/Activitati/padurile-au-nevoie-de-voluntari/ (accessed 3.19.16).

Griffith, P., Kuemmerle, T., Knorn, J., Hostert, P., Kennedy, R.E., Abrudan, I. V, 2012. Using annual time-series of Landsat images to assess the effects of forest restitution in 118, 199–214.

Hamunyela, E., Verbesselt, J., Herold, M., 2016. Using spatial context to improve early detection of deforestation from Landsat time series. Remote Sens. Environ. 172, 126–138.

Hansen, M.C., Potapov, P. V, Moore, R., Hancher, M., Turubanova, S. a, Tyukavina, a, Thau, D., Stehman, S. V, Goetz, S.J., Loveland, T.R., Kommareddy, a, Egorov, a, Chini, L., Justice, C.O., Townshend, J.R.G., 2013. High-resolution global maps of 21st-century forest cover change. Science 342, 850–3.

Harris Geospatial, 2016. Spectral Indices (Using ENVI) | Exelis VIS Docs Center . URL https://www.harrisgeospatial.com/docs/SpectralIndices.html (accessed 4.16.16).

Hermosilla, T., Wulder, M.A., White, J.C., Coops, N.C., Hobart, G.W., 2015. Regional detection, characterization, and attribution of annual forest change from 1984 to 2012 using Landsat-derived time-series metrics. Remote Sens. Environ. 170, 121–132.

Huete, A., Didan, K., Miura, T., Rodriguez, E.P., Gao, X., Ferreira, L.G., 2002. Overview of the radiometric and biophysical performance of the MODIS vegetation indices. Remote Sens. Environ. 83, 195–213.

Hutchinson, J.M.S., Jacquin, A., Hutchinson, S.L., Verbesselt, J., 2015. Monitoring vegetation change and dynamics on U.S. Army training lands using satellite image time series analysis. J. Environ. Manage. 150, 355–366.

Introduction to bfastSpatial, 2016. Introduction to bfastSpatial . URL http://www.loicdutrieux.com/bfastSpatial/ (accessed 5.11.16).

ISU Covasna, 2014. Planul de analiză și acoperire a riscurilor al județului Covasna. PhD Propos. 1, 1–42.

Keenan, R.J., Reams, G.A., Achard, F., de Freitas, J. V., Grainger, A., Lindquist, E., 2015. Dynamics of global forest area: Results from the FAO Global Forest Resources Assessment 2015. For. Ecol. Manage. 352, 9–20.

Kennedy, R.E., Yang, Z., Cohen, W.B., 2010. Detecting trends in forest disturbance and recovery using yearly Landsat time series: 1. LandTrendr - Temporal segmentation algorithms. Remote Sens. Environ. 114, 2897–2910.

Knorn, J., Kuemmerle, T., Radeloff, V.C., Szabo, A., Mindrescu, M., Keeton, W.S., Abrudan, I., Griffiths, P., Gancz, V., Hostert, P., 2012. Forest restitution and protected area effectiveness in post-socialist Romania. Biol. Conserv. 146, 204–212.

Lambert, J., Denux, J.-P., Verbesselt, J., Balent, G., Cheret, V., 2015. Detecting Clear-Cuts and Decreases in Forest Vitality Using MODIS NDVI Time Series. Remote Sens. 7, 3588–3612.

Lambert, J., Drenou, C., Denux, J., Balent, G., Cheret, V., 2013. Monitoring forest decline through remote sensing time series analysis. GIScience Remote Sens. 50, 437–457.

Landsat USGS, 2016a. USGS.gov | Science for a changing world . URL https://www.usgs.gov/ (accessed 5.12.16).

Landsat USGS, 2016b. Landsat Surface Reflectance High Level Data Products . URL http://landsat.usgs.gov/CDR_LSR.php (accessed 3.27.16).

Law 46/2008, n.d. LEGE - nr.46 din 19 martie 2008 Codul silvic . URL http://www.cdep.ro/pls/legis/legis_pck.htp_act?ida=78532 (accessed 5.12.16).

Lawrence, A., Nicoll, B., 2016. limate Impacts and Adaptations in Forest Management, Second Edi. ed, Climate Change. Elsevier B.V.

MacDicken, K.G., 2015. Global Forest Resources Assessment 2015: What, why and how? For. Ecol. Manage. 352, 3–8.

Mediafax, 2016. Radarul pădurilor . URL http://www.mediafax.ro/social/radarul-padurilor-oricine-va-putea-cere-verificarea-legalitatii-unui-transport-de-lemn-apeland-112-video-13351623 (accessed 3.19.16).

Merce, O., 2012. Natura 2000 and the forests in Romania – management principles , problems and threats. J. Hortic. For. Biotechnol. 16, 139–144.

Mihășan, C.D., 2009. Sustainable management of forest area in Romania.

Ministry of Environment and Climate Change Romania, 2016. Paduri | Ministerul

Mediului, Apelor si Padurilor . URL http://www.mmediu.ro/categorie/paduri/25 (accessed 3.15.16).

Munteanu, C., Nita, M.D., Abrudan, I.V., Radeloff, V.C., 2016. Historical forest management in Romania is imposing strong legacies on contemporary forests and their management. For. Ecol. Manage. 361, 179–193.

National Cartography Center History, 2016. Istoric Centrul Național de Cartografie . URL http://www.cngcft.ro/index.php/features/scurt-istoric (accessed 4.15.16).

National Institute of Statistics, 2016a. Geografie . URL http://www.covasna.insse.ro/main.php?id=405 (accessed 3.21.16).

National Institute of Statistics, 2016b. INSSE - Baze de date statistice - TEMPO-Online serii de timp . URL http://statistici.insse.ro/shop/ (accessed 4.14.16).

Nostra Silva, 2016. Rezultatele Inventarului Forestier National - Nostra Silva . URL http://www.nostrasilva.ro/activitati/rezultatele-inventarului-forestier-national/ (accessed 4.13.16).

Pfaff, A., Amacher, G.S., Sills, E.O., Coren, M.J., Streck, C., Lawlor, K., 2013. Deforestation and Forest Degradation: Concerns, Causes, Policies, and Their Impacts, 1st ed, Encyclopedia of Energy, Natural Resource, and Environmental Economics. Elsevier Inc.

PRODES, 2016. Projeto - PRODES . URL http://www.obt.inpe.br/prodes/index.php (accessed 4.8.16).

Ramsey, F., 2012. e-Study Guide for: The Statistical Sleuth: A Course in Methods of Data Analysis, Content Technologies, ISBN 9781467275514.

Reiche, J., Verbesselt, J., Hoekman, D., Herold, M., 2015. Fusing Landsat and SAR time series to detect deforestation in the tropics 156, 276–293.

RoSilva, 2016. www.sfgh.rosilva.ro . URL http://sfgh.rosilva.ro/articole/prezentare_generala__p_1151.htm (accessed 3.26.16).

Schultz, M., Verbesselt, J., Avitabile, V., Souza, C., Herold, M., 2015. Error Sources in Deforestation Detection Using BFAST Monitor on Landsat Time Series Across Three Tropical Sites. IEEE J. Sel. Top. Appl. Earth Obs. Remote Sens.

The REDD Desk, 2016. What is REDD+? | The REDD Desk . URL http://theredddesk.org/what-redd (accessed 3.19.16).

Tran, T. V., de Beurs, K.M., Julian, J.P., 2016. Monitoring forest disturbances in Southeast Oklahoma using Landsat and MODIS images. Int. J. Appl. Earth Obs. Geoinf. 44, 42–52.

Tsutsumida, N., Saizen, I., Matsuoka, M., Ishii, R., 2013. Land Cover Change Detection in Ulaanbaatar Using the Breaks for Additive Seasonal and Trend Method. Land 2, 534–549.

USGS, 2015. Product Guide: Landsat Surface Reflectance-Derived Spectral Indices.

Verbesselt, J., Hyndman, R., Newnham, G., Culvenor, D., 2010a. Detecting trend and

seasonal changes in satellite image time series. Remote Sens. Environ. 114, 106–115.

Verbesselt, J., Hyndman, R., Zeileis, A., Culvenor, D., 2010b. Phenological change detection while accounting for abrupt and gradual trends in satellite image time series. Remote Sens. Environ. 114, 2970–2980.

Verbesselt, J., Kalomenopoulos, M., Souza, C., Herold, M., 2012a. Near real-time deforestation monitoring in tropical ecosystems using satellite image time series 2020–2023.

Verbesselt, J., Zeileis, A., Herold, M., 2012b. Near real-time disturbance detection using satellite image time series. Remote Sens. Environ. 123, 98–108.

Watercore, 2016. Water Core: Water scarcity and droughts; coordinated actions in European regions" . URL http://www.watercore.eu/covasna.asp (accessed 3.21.16).

Watts, L.M., Laffan, S.W., 2014. Effectiveness of the BFAST algorithm for detecting vegetation response patterns in a semi-arid region. Remote Sens. Environ. 154, 234–245.

Willis, K.J., 1994. the Vegetational History of the Balkans 13, 769–788.

Willis, K.J., 2009. Evolution and Function of Earth's Biomes: Temperate Forests. Earth Syst. Hist. Nat. Var. Vol. III III.

WWF, 2016. Păduri | WWF . URL http://www.wwf.ro/ce_facem/paduri/ (accessed 5.5.16).

WWF Danube Carpathian Programme, 2005. Illegal Logging in Romania 17.

Zhu, Z., Wang, S., Woodcock, C.E., 2015. Improvement and expansion of the Fmask algorithm: Cloud, cloud shadow, and snow detection for Landsats 4-7, 8, and Sentinel 2 images. Remote Sens. Environ. 159, 269–277.

Zhu, Z., Woodcock, C.E., 2012. Object-based cloud and cloud shadow detection in Landsat imagery. Remote Sens. Environ. 118, 83–94.

Appendix A: Used software

The forest mask, the pre-processing of the Landsat data, the BFAST analysis and the random sampling were performed in R environment (Version 0.99.879, RStudio Inc., Boston, United States). Visual interpretation was conducted using Google Earth Pro (Version 7.1.2.2041, Google Inc., California, United States), the maps were produced with Esri ArcMap (Version 10.1, Build 3035, Environmental Systems Research Institute, Inc., California, United States) and the graphs, tables and the writing process have been done using Microsoft Office Professional Plus (Version 14.0.6112.5000, Microsoft Corporation, Washington, United States).
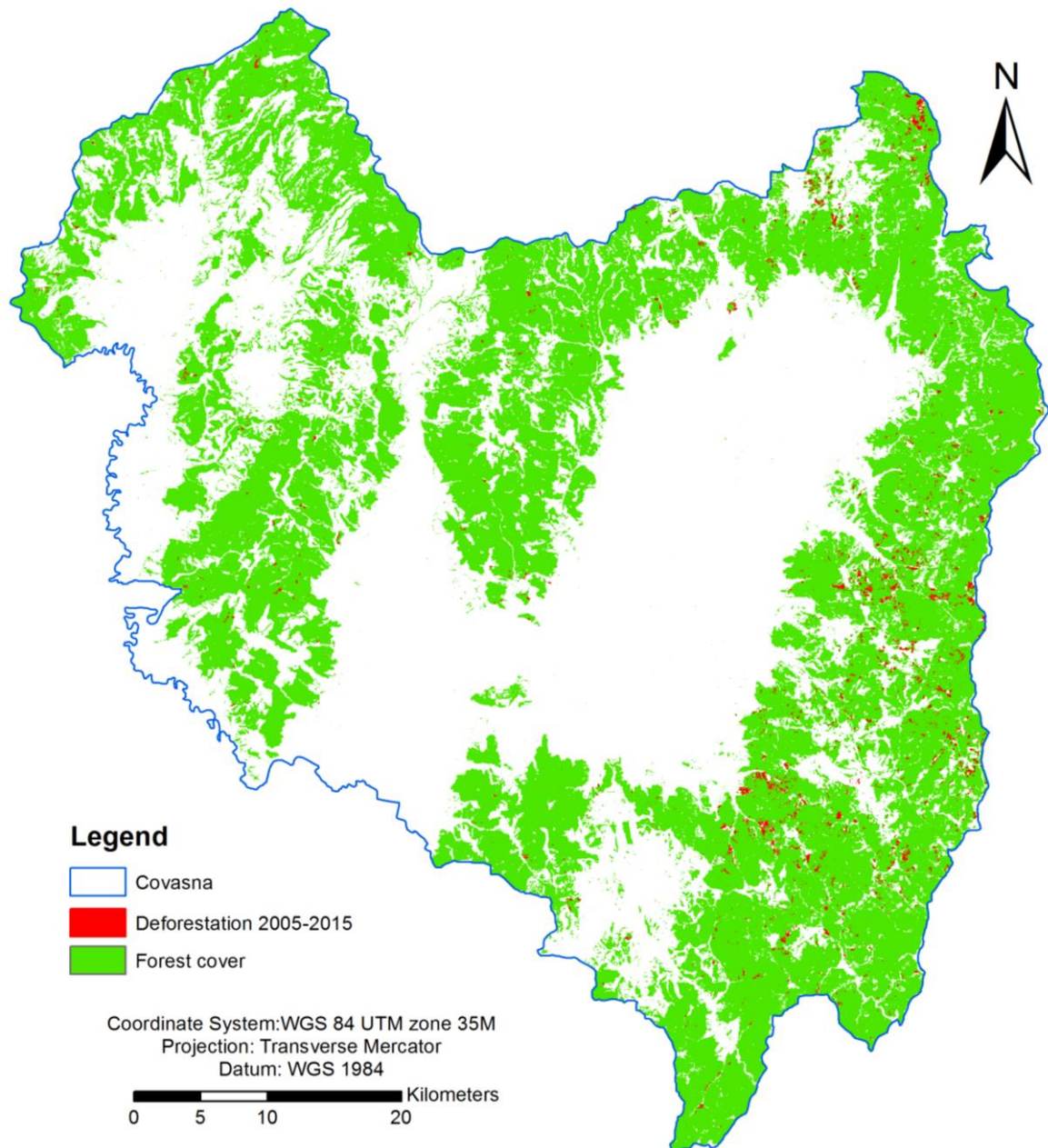
Appendix B: Threshold selection

This table indicates how the decision regarding the NDMI threshold has been made. It shows only a part of the complete NDMI table. This table is sorted by magnitude. The columns of the table represent as follows: the number of each of the randomly selected points, the year when the break was detected, the magnitude and the decision (True or False) based on Google Earth visual interpretation. First, every random point was checked with Google Earth images, and a value (True or False) was assigned to each random point as follows: if clear-cut deforestation occurred the T value was assigned and if other type of change was detected, the point was assigned the F value. Then, every two points were grouped depending on their values (i.e. if both points were True, the resulting value was True; if both points were False, the resulting value was False; if one point was True and the other was False, the resulting value was True/False). The next group was made in the same way, with the mention that if a True/False was grouped with a T value, then the resulting value was True and if a True/False value was grouped with an F value, then the resulting value was False. After this step was done, a threshold was defined based on the interval (i.e. -942.388 -844.096) where the True and False values did not lead to a straightforward decision. Considering that a threshold value was needed, an integer value was selected from the interval (i.e. -850). The values which were smaller than -850 were considered clear-cut deforestation. The threshold for NDVI was determined in the same way (i.e. -350).

No. of pixels	Year	Magnitude	Decision				
13	2008.222	-1050.246	T	T	T	T	T
78	2005.858	-1045.105	T				
41	2010.589	-1027.969	T	T			
73	2007.304	-1019.301	T				
35	2010.808	-1015.632	T	T	FT		
3	2010.326	-1009.370	T				
7	2010.677	-1009.037	F	F			
76	2007.041	-1004.815	F				
29	2011.247	-985.867	T	FT	F	FT	
5	2007.260	-981.954	F				
97	2008.222	-972.216	F	F			
94	2008.441	-969.676	F				
44	2008.529	-962.110	T	T			
55	2005.858	-945.267	T				
22	2007.567	-943.598	F	FT			
62	2007.304	-942.528	T				
70	2010.808	-942.388	F	F	FT	F	FT
51	2007.304	-930.438	F				
54	2009.318	-922.297	T	T			
21	2009.318	-910.904	T				
85	2007.304	-906.676	F	F	F		
15	2010.589	-903.430	F				
45	2005.858	-901.084	T	FT			
9	2009.318	-890.432	F				
37	2010.808	-878.666	T	T	FT	T	
39	2007.304	-876.862	T				
67	2010.677	-865.920	F	F			
11	2008.836	-860.832	F				
96	2011.247	-857.481	F	FT	T		
92	2007.260	-851.986	T				
25	2006.559	-844.223	T	T			
61	2007.304	-844.096	T				
68	2007.304	-842.648	F	F	F	F	F
6	2008.222	-830.706	F				
1	2007.786	-829.588	F	F			
38	2007.786	-829.081	F				
59	2007.655	-824.990	T	FT	FT		
36	2008.266	-818.594	F				
23	2007.304	-806.902	F	FT			
2	2006.647	-798.442	T				
9	2009.318	-794.381	F	FT	FT	FT	
4	2007.260	-773.045	T				
8	2011.247	-764.159	T	FT			
26	2007.304	-742.727	F				
40	2008.266	-742.412	F	FT	FT		
12	2007.567	-722.106	T				
60	2007.260	-720.732	T	FT			
100	2007.655	-712.782	F				

Appendix C:

Map of clear-cut deforestation (BFAST final results) in Covasna County, Romania. The blue line represents the Covasna County boundaries, the green area indicates the forest cover in 2005 from the GFW database and the red areas represent the clear-cut deforestation

Legend

☐ Covasna

■ Deforestation 2005-2015

■ Forest cover

Coordinate System:WGS 84 UTM zone 35M
Projection: Transverse Mercator
Datum: WGS 1984

0   5   10   20   Kilometers

52

Institutionen för naturgeografi och ekosystemvetenskap, Lunds Universitet.

Student examensarbete (Seminarieuppsatser). Uppsatserna finns tillgängliga på institutionens geobibliotek, Sölvegatan 12, 223 62 LUND. Serien startade 1985. Hela listan och själva uppsatserna är även tillgängliga på LUP student papers (https://lup.lub.lu.se/student-papers/search/) och via Geobiblioteket (www.geobib.lu.se)

The student thesis reports are available at the Geo-Library, Department of Physical Geography and Ecosystem Science, University of Lund, Sölvegatan 12, S-223 62 Lund, Sweden. Report series started 1985. The complete list and electronic versions are also electronic available at the LUP student papers (https://lup.lub.lu.se/student-papers/search/) and through the Geo-library (www.geobib.lu.se)

350   Mihaela – Mariana Tudoran (2015) Occurrences of insect outbreaks in Sweden in relation to climatic parameters since 1850

351   Maria Gatzouras (2015) Assessment of trampling impact in Icelandic natural areas in experimental plots with focus on image analysis of digital photographs

352   Gustav Wallner (2015) Estimating and evaluating GPP in the Sahel using MSG/SEVIRI and MODIS satellite data

353   Luisa Teixeira (2015) Exploring the relationships between biodiversity and benthic habitat in the Primeiras and Segundas Protected Area, Mozambique

354   Iris Behrens & Linn Gardell (2015) Water quality in Apac-, Mbale- & Lira district, Uganda - A field study evaluating problems and suitable solutions

355   Viktoria Björklund (2015) Water quality in rivers affected by urbanization: A Case Study in Minas Gerais, Brazil

356   Tara Mellquist (2015) Hållbar dagvattenhantering i Stockholms stad - En riskhanteringsanalys med avseende på långsiktig hållbarhet av Stockholms stads dagvattenhantering i urban miljö

357   Jenny Hansson (2015) Trafikrelaterade luftföroreningar vid förskolor – En studie om kvävedioxidhalter vid förskolor i Malmö

358   Laura Reinelt (2015) Modelling vegetation dynamics and carbon fluxes in a high Arctic mire

359   Emelie Linnéa Graham (2015) Atmospheric reactivity of cyclic ethers of relevance to biofuel combustion

360   Filippo Gualla (2015) Sun position and PV panels: a model to determine the best orientation

361   Joakim Lindberg (2015) Locating potential flood areas in an urban environment using remote sensing and GIS, case study Lund, Sweden

362   Georgios-Konstantinos Lagkas (2015) Analysis of NDVI variation and snowmelt around Zackenberg station, Greenland with comparison of ground data and remote sensing.

363   Carlos Arellano (2015) Production and Biodegradability of Dissolved Organic Carbon from Different Litter Sources

364   Sofia Valentin (2015) Do-It-Yourself Helium Balloon Aerial Photography - Developing a method in an agroforestry plantation, Lao PDR

365   Shirin Danehpash (2015) Evaluation of Standards and Techniques for Retrieval of Geospatial Raster Data - A study for the ICOS Carbon Portal

366   Linnea Jonsson (2015) Evaluation of pixel based and object based classification methods for land cover mapping with high spatial resolution satellite imagery, in the Amazonas, Brazil.

367   Johan Westin (2015) Quantification of a continuous-cover forest in Sweden using remote sensing techniques

368   Dahlia Mudzaffar Ali (2015) Quantifying Terrain Factor Using GIS Applications for
Real Estate Property Valuation

369   Ulrika Belsing (2015) The survival of moth larvae feeding on different plant species in northern Fennoscandia

370   Isabella Grönfeldt (2015) Snow and sea ice temperature profiles from satellite data and ice mass balance buoys

371   Karolina D. Pantazatou (2015) Issues of Geographic Context Variable Calculation Methods applied at different Geographic Levels in Spatial Historical Demographic Research -A case study over four parishes in Southern Sweden

372   Andreas Dahlbom (2016) The impact of permafrost degradation on methane fluxes - a field study in Abisko

373   Hanna Modin (2016) Higher temperatures increase nutrient availability in the High Arctic, causing elevated competitive pressure and a decline in *Papaver radicatum*

374   Elsa Lindevall (2016) Assessment of the relationship between the Photochemical Reflectance Index and Light Use Efficiency: A study of its seasonal and diurnal variation in a sub-arctic birch forest, Abisko, Sweden

375   Henrik Hagelin and Matthieu Cluzel (2016) Applying FARSITE and Prometheus on the Västmanland Fire, Sweden (2014): Fire Growth Simulation as a Measure Against Forest Fire Spread – A Model Suitability Study –

376   Pontus Cederholm (2016) Californian Drought: The Processes and Factors Controlling the 2011-2016 Drought and Winter Precipitation in California

377   Johannes Loer (2016) Modelling nitrogen balance in two Southern Swedish spruce plantations

378   Hanna Angel (2016) Water and carbon footprints of mining and producing Cu, Mg and Zn: A comparative study of primary and secondary sources

379   Gusten Brodin (2016) Organic farming's role in adaptation to and mitigation of climate change - an overview of ecological resilience and a model case study

380   Verånika Trollblad (2016) Odling av *Cucumis Sativus* L. med aska från träd som näringstillägg i ett urinbaserat hydroponiskt system

381   Susanne De Bourg (2016) Tillväxteffekter för andra generationens granskog efter tidigare genomförd kalkning

382   Katarina Crafoord (2016) Placering av energiskog i Sverige - en GIS analys

383   Simon Nåfält (2016) Assessing avalanche risk by terrain analysis An experimental GIS-approach to The Avalanche Terrain Exposure Scale (ATES)

384   Vide Hellgren (2016) Asteroid Mining - A Review of Methods and Aspects

385   Tina Truedsson (2016) Hur påverkar snömängd och vindförhållande vattentrycksmätningar vintertid i en sjö på västra Grönland?

386   Chloe Näslund (2016) Prompt Pediatric Care Pediatric patients' estimated travel times to surgically-equipped hospitals in Sweden's Scania County

387 Yufei Wei (2016) Developing a web-based system to visualize vegetation trends by a nonlinear regression algorithm

388 Greta Wistrand (2016) Investigating the potential of object-based image analysis to identify tree avenues in high resolution aerial imagery and lidar data

389 Jessica Ahlgren (2016) Development of a Web Mapping Application for grazing resource information in Kordofan, Sudan, by downloading MODIS data automatically via Python

390 Hanna Axén (2016) Methane flux measurements with low-cost solid state sensors in Kobbefjord, West Greenland

391 Ludvig Forslund (2016) Development of methods for flood analysis and response in a Web-GIS for disaster management

392 Shuzhi Dong (2016) Comparisons between different multi-criteria decision analysis techniques for disease susceptibility mapping

393 Thirze Hermans (2016) Modelling grain surplus/deficit in Cameroon for 2030

394 Stefanos Georganos (2016) Exploring the spatial relationship between NDVI and rainfall in the semi-arid Sahel using geographically weighted regression

395 Julia Kelly (2016) Physiological responses to drought in healthy and stressed trees: a comparison of four species in Oregon, USA

396 Antonín Kusbach (2016) Analysis of Arctic peak-season carbon flux estimations based on four MODIS vegetation products

397 Luana Andreea Simion (2016) Conservation assessments of Văcărești urban wetland in Bucharest (Romania): Land cover and climate changes from 2000 to 2015

398 Elsa Nordén (2016) Comparison between three landscape analysis tools to aid conservation efforts

399 Tudor Buhalău (2016) Detecting clear-cut deforestation using Landsat data: A time series analysis of remote sensing data in Covasna County, Romania between 2005 and 2015